Ecological Indicators 122 (2021) 107304

Contents lists available at ScienceDirect

Ecological Indicators

journal homepage: www.elsevier.com/locate/ecolind

Mechanisms influencing particle depletion in and around mussel farms in different environments

Daniel Taylor [a,*], Janus Larsen [b], Anna-Lucia Buer [c], Rene Friedland [c], Andreas Holbach [b], Jens Kjerulf Petersen [a], Pernille Nielsen [a], Lukas Ritzenhofen [c,d], Camille Saurel [a], Marie Maar [b]

[a] Section for Coastal Ecology, National Institute of Aquatic Resources, DTU Aqua, Nykøbing-Mors, Denmark
[b] Aarhus University, Department of Bioscience, Roskilde, Denmark
[c] Leibniz-Institute for Baltic Sea Research Warnemünde, Rostock, Germany
[d] Marine Research Institute, Klaipeda University, Klaipeda, Lithuania

ARTICLE INFO

Keywords:
Western Baltic Sea
Chlorophyll
Water transparency
Secchi depth
Mussel farming
Eutrophication

ABSTRACT

Through the mechanisms of particle immobilization and subsequent depletion of particles, mussel cultivation has a direct effect on chlorophyll-a concentrations and Secchi depth; both of which are primary indicators of marine ecological status and metrics for water quality management. As such, mussel cultivation has been proposed as a measure to mitigate the effects of coastal eutrophication. However, the extent to which this ecosystem service, and relatedly, biomass accumulation, are affected by ambient environmental conditions involves complex interactions. To explore the interacting mechanisms underpinning depletion dynamics under various biophysical conditions along the salinity gradient in the Baltic Sea, we used an updated Dynamic Energy Budget (DEB) model with field data from the western Baltic Sea, accommodating osmotic stress. We use the DEB model to drive a 3D farm-scale model within a novel precompiled hydrodynamic framework (FlexSem) to evaluate the effects of different environmental conditions and farm configuration on the intensity and extent of the chlorophyll-a depletion signal. We also report on extensive *in situ* monitoring of chlorophyll-a and Secchi depth within and around mussel farms, from several cultivation areas from around the western Baltic Sea to evaluate site-specific characteristics of depletion. Monitoring reflected the high degree of spatio-temporal variability in the quantification of this ecosystem service; with relative differences in chlorophyll-a from −14 to 69% and Secchi depth from 0 to 75%. We find that the extensive *in situ* measurements in different environmental conditions can be represented by the integrated farm model in terms of mussel biomass accumulation and depletion, providing insight on the interactions of current velocity, farm orientation to predominant current direction, ambient chlorophyll-a concentrations, and total biomass loads on the intensity and spatial extent of the depletion signal. Furthermore, the model has been calibrated to cover a variety of environmental contexts and permits fine-resolution simulation of multiple environmental interactions on mussel energetics, which can be used to evaluate potentials for optimizing mussel mitigation culture and the associated ecosystem services of phytoplankton depletion under local conditions without extensive recalibration from field growth data. The general interactions exhibited here and model will be useful for evaluating depletion and planning the establishment of mitigation farms in regions where national environmental monitoring programs can provide basic data. This can also reduce the need for extensive and costly *in situ* monitoring programs.

1. Introduction

The impacts of eutrophication on coastal ecosystems have been widely documented over the past decades, where some of the most representative and easily measurable symptoms include increased phytoplankton concentrations and concomitant decreased water clarity (Bricker et al., 2003, 2014; Ferreira et al., 2011). In concerted efforts to improve anthropogenic eutrophication, inter-state agreements have been implemented around the world, designed to reduce nutrient loads on the coastal environment; such as the Baltic Sea Action Plan (BSAP, HELCOM, 2007, 2013) in 2007 (Backer et al., 2010), and the Water Framework Directive (WFD, 2000/60/EC) in 2000 for all European

* Corresponding author at: Ørroddevej 80, 7900 Nykøbing Mors, Denmark.
E-mail address: dtay@aqua.dtu.dk (D. Taylor).

https://doi.org/10.1016/j.ecolind.2020.107304
Received 8 September 2020; Received in revised form 13 December 2020; Accepted 19 December 2020
Available online 30 December 2020

inland and coastal water bodies to reach "Good Ecological Status" by the current decade (Borja et al., 2013). While many immediate successes were realized in the reduction of nutrient loads (Boesch, 2019), many coastal ecosystems, including the majority of Baltic waters, are still eutrophic (Kristensen et al., 2018), and further abatement will require multiple, combined measures (Duarte and Krause-Jensen, 2018; Friedland et al., 2019b). As one of only a few instruments to mitigate eutrophication within the marine environment (Petersen et al., 2019a), mussel farming (*Mytilus* spp.) in suspended culture is progressing as a novel mechanism. An assortment of ecosystem services fundamentally arises out of the filtration mechanism, which immobilizes large fractions of suspended organic matter from the water column (Petersen et al., 2019b; Strand and Ferreira, 2019). This is often quantified by a combination of methods, commonly, chlorophyll-a concentration (chl-a), and Secchi depth, as they are complimentary measures to summarize the manifold effects of high seston concentrations on aquatic ecology and direct indicators of eutrophication effects (Fleming-Lehtinen and Laamanen, 2012; Fleming-Lehtinen et al., 2015). As key indicators in the WFD assessment of ecological status, chl-a and Secchi depth are useful measures to demonstrate the ecological feasibility of mussel cultivation for acceptance as a mitigation tool in different environmental conditions around the Baltic Sea, as the indicators are directly related to the food resources exploited by mussels.

When bivalve filtration ('grazing pressure') outpaces phytoplankton turnover, as is common in mussel farms, food depletion occurs. The depletion effect is a common feature of bivalve aggregates, and has most often been reported at a multitude of scales in space and time across a variety of environments and species (Cranford, 2019; Hulot et al., 2018). Measuring a depletion signal at the meso (farm) and macro-scale (basin, domain) has proven often difficult and highly variable, provided the array of various interacting biophysical conditions, seston composition, and the configuration of bivalve aggregations (Petersen et al., 2019b). Mechanisms associated with depletion specific to mussel farming have principally been studied in a piecewise manner, but have been described in relation to physical particle dynamics and particle filtration in a complex 3D setting (Cranford et al., 2011; Cranford, 2019), which further makes comparison between depletion studies difficult. In addition to ambient biophysical dynamics, mussel filtration is mediated by particle composition, and concentrations, where capture efficiency declines precipitously with smaller particles (<4μm ESD, (Møhlenberg and Riisgård, 1978; Cranford et al., 2016; Rosa et al., 2018)) and filtration is negligible below 0.5 μg l^{-1} chl-a in most coastal regions (Dolmer, 2000; Riisgård et al., 2003). This is a broad generalization, as bivalve filtration functions across the spectrum of seston constituents (i.e. detritus, bacterial aggregates, zooplankton), and particle-size limitation is dependent on shape, aggregation, and surface chemistry (Cranford et al., 2011; Cranford, 2019; Gosling, 2015; Rosa et al., 2018). Nevertheless, the equivalent size (μm) and limiting concentration are useful thresholds as the majority of food particles are larger phytoplankton for suspended bivalves in eutrophic waters (Cloern, 2018). Filtration capacity of a farm is furthermore regulated by aggregate numbers and size of mussels, and energetics, which is driven by ambient environmental conditions, such as salinity (Buer et al., 2020). In general, studies have tended to evaluate depletion at limited scales, employing a variety of approaches to quantify seston concentrations within and around mussel farming structures that typically rely on discrete sampling or continuous point-based measurements, which can be difficult to generalize by environmental context, mussel cultivation strategy, or measurement approach. Models describing the effects of suspension feeding on seston concentrations are useful for evaluating the biophysical properties of food flux and relative depletion of food, which can furthermore inform on optimal farm layout and mussel stocking density (Friedland et al., 2019a) or in itself serve as an ecological indicator of carrying capacity (Gibbs, 2007). *In situ* measurements are necessary to validate our confidence in models, however, they are often difficult to repeatedly conduct, are expensive, and are susceptible to error propagation (Jansen et al., 2016). In addition to measurement error, *in situ* measurements are burdened by attempting to quantify a dynamic medium that is constantly changing in space and time.

Depletion modeling and field study has typically been constrained to limited spatial and environmental variation (Newell et al., 2019); particularly in regards to salinity and eutrophic condition. Regional-scale modeling of mitigation potential is far too coarse to resolve the implications of hydrodynamics and local environmental conditions on farm-scale production and depletion dynamics (Holbach et al., 2020). Modeling mussel growth and seston depletion at the farm-scale has largely developed along perspectives of carrying capacity for optimal management and production of mussels directed to the human consumption market; e.g. the FARM model, ShellGIS (Ferreira et al., 2007; Newell et al., 2013); with rare examples evaluating the process as an ecosystem service (i.e. Nielsen et al., 2016). Varying in complexity and intended purpose, models addressing carrying capacity and the relationship to environmental conditions have been important for both farmers and water quality managers with applications at multiple scales (Grant and Filgueira, 2011). As the mussel mitigation concept may be applied across the gradient of environmental conditions in the Baltic Sea, it is important to characterize the interaction of this environmental service under variable conditions with relatively simple inputs. Likewise, to maximize nutrient mitigation within these variable conditions, modifications in farm configuration relating to food flux and depletion can be accomplished by running model scenarios.

The aim of the present study was to quantify depletion by evaluating the degree of influence of multiple environmental drivers on chl-*a* depletion (field and model data) and Secchi depth (field data) around mussel farms in different environments. We develop a simple 3D farm-scale model that integrates an updated Dynamic Energy Budget (DEB) model, a population function, and environmental drivers in an open source hydrodynamic framework. The model is used to simulate particle depletion under different configurations and explore mechanisms influencing the spatial structure of depletion and the intensity of the depletion signal under scenarios representative of Baltic environmental conditions. The model estimations were contrasted with multiple extensive *in situ* measurements of chl-a depletion and Secchi depth improvements to evaluate relative depletion of food. Furthermore, a spatial statistical approach was employed to two sites to assess the extent and intensity of *in situ* depletion in high resolution transects. From these combined findings, we explore how general interactions of cultivation and environmental conditions can influence management and implementation of mitigation mussel farming.

2. Materials and method

2.1. Study areas

2.1.1. Depletion monitoring sites

We present depletion data from six areas in the western Baltic (locations: Fig. 1, methods: Table 1) with different environmental conditions and two modes of suspended mussel cultivation and use a farm-scale model at one site with various biophysical scenarios. Representative average environmental conditions of the farm sites (temperature, salinity, chl-a) within each area can be seen in Figure A.1. Average measured environmental conditions for each site over their respective monitoring periods are presented in Table 2. Configurations of farms are outlined in the appendix, Table A.1. Farms were either equipped with conventional longlines (LL with spat collectors) or tube-nets (TN), which consist of a floating plastic tube supporting a 3 m net; see Taylor et al. (2019) for further detail.

The Limfjorden system (Fig. 1) separates northern Jutland from mainland Jutland with openings at the North Sea and Kattegat. It is a shallow (average 4.8 m) system of semi-enclosed estuaries with salinity gradients according to freshwater inputs (2.7 10^9 m^3 annually) from the 7528 km^2 catchment and exchange with the adjacent seas (Hofmeister

Fig. 1. Overview map of DEB calibration sites (blue circles) and depletion monitoring sites (orange squares). (For interpretation of the references to colour in this figure legend, the reader is referred to the web version of this article.)

Table 1
Overview of the sampling locations. Name, location, farming period, water depth, farm size, standing mussel biomass at late autumn/early winter sampling (except for GWB in June 2018), and methods used to detect depletion.

Station	Location	Period	Water depth (m)	Farm size (ha)	Mussel biomass (t-WW)	Point data	Continuous transect
Venø Sund	Limfjorden, Denmark	Jun 2018 – December 2019	4–6	74	5000–6000 (10/19)	monthly	√
Sallingsund	Limfjorden, Denmark	Jun 2017 – Apr 2018; Jun 2018 – Apr 2019	5–7	14.8	100–150 (12/2018,19)	monthly	χ
Dråby Vig	Limfjorden, Denmark	Jun 2017 – Apr 2018; Jun 2018 – Jan 2019	5–7	23.1	220 (12/17) 170 (12/18)	monthly	√
Skive Fjord	Limfjorden, Denmark	Jun 2017 – Dec 2017; Jun 2018 – Nov 2018	5–6	21.9	573 (12/17) 507 (11/18)	monthly	√
As Vig	Horsens Fjord, Denmark	May 2018-Oct 2018	10–12	11.3	729 (10/18)	monthly	χ
Greifswald Bay	Germany	Jun 2017 - Oct 2018	5–6	0.3	2 (6/18)	monthly	χ

Table 2
Averages of ambient current speed during the monitoring period, temperature, salinity and chl-a concentrations during the sampling periods. *From ADCP data. n.m. = not measured.

Station	Current speeds (cm s^{-1})	Average temperature (°C)	Average salinity (PSU)	Average chl-a conc. (µg l^{-1})	Secchi depths (m)
Venø Sund	1.99 ± 0.86	16.0 ± 3.7	29.5 ± 0.8	6.46 ± 2.09	3.61 ± 0.52
Sallingsund	2.03 ± 0.74	11.8 ± 7.1	29.8 ± 1.9	3.58 ± 2.33	2.58 ± 0.62
Dråby Vig	1.34 ± 0.37	13.7 ± 5.5	28.0 ± 1.2	3.56 ± 1.74	3.17 ± 1.22
Skive Fjord	1.10 ± 0.40	12.0 ± 7.0	24.0 ± 1.4	5.49 ± 2.76	3.34 ± 1.39
As Vig	7.76 ± 3.24*	13.4 ± 4.1	24.0 ± 2.0	2.39 ± 0.88	4.75 ± 0.29
Greifswald Bay	1.64 ± 0.75*	16.7 ± 5.2	6.9 ± 0.7	12.6 ± 8.1	2.40 ± 0.71
Latvia	n.m.	12.0 ± 6.0	6.9 ± 0.2	2.6 ± 1.3	n.m.

et al., 2009). The system is classified as in poor ecological condition by WFD standards, experiences periodic hypoxic events due to persistent eutrophic conditions, and has a relatively high internal load of nutrients (Conley et al., 2011; Miljø- og Fødevareministeriet, 2016).

Mussel farming is relatively new in the Limfjorden, with the industry taking hold in the beginning of the millennium, but is the most productive region in Denmark at >4500 t of mussels annually for the fresh market. Four existing commercial mussel farms were monitored between 2017 and 2019 (Fig. 1). All farms are normally configured for production of high-quality mussels specific for the human consumption market using LL, with the exception of the Venø Sund farm, using TN and the first mitigation farm in operation in the Limfjorden since 2018. The farm in Venø Sund is the largest in Denmark, situated by the western shores of a small sound in the western Limfjorden, roughly aligned with the predominant south-north longshore currents. The Sallingsund farm is a medium-sized farm of which about half is normally used, and typically experiences higher current velocities than the other farms in the Limfjorden due to the narrowing of the sound between the island of Mors and the mainland. The Dråby Vig site experiences larger circulation patterns interacting with the bay topography and the neighboring Løgstør Broad, but otherwise similar conditions to Sallingsund. These three sites have typically higher salinity than all other sites (27–30 PSU). The Skive Fjord site experiences relatively higher concentrations of chl-a, but lower salinity (23–25 PSU) and current magnitudes than the other Limfjorden sites. Limited portions of farms were used in the 2017–2018 production seasons for testing of mitigation production, as described in Taylor et al. (2019). In the 2018 season, the central section of the Skive Fjord site was replaced with 20 tube-nets, while only 4 were placed in the NE corner of Dråby Vig site. It should be noted that tube-nets have much higher surface area per unit water column volume than traditional spat collectors and host significantly higher aggregations of mussels (Taylor et al., 2019).

As Vig is an exposed cove in eastern Jutland in the southwestern Kattegat. This site is representative of open Kattegat waters, with higher current velocities (Table 2) and wave exposure than the other sites, moderately high salinity (24–26 PSU), deeper (10–12 m), and is host to several fish farm operations. The site was monitored between the summer of 2017 until the winter of 2018/19 after harvest, while primary settlement occurred in October of 2017 and May 2018.

Greifswald Bay (GWB) is a shallow inshore basin located in the north east of Germany, with an average water depth of 5.8 m. It is limited by the mainland in the south and the Island of Rügen in the West (Mecklenburg-Western Pomerania). GWB is connected with the Baltic Sea by a wide and shallow opening to the east and a narrow sound (Strelasund) in the west. Salinity levels range from 6 to 8 PSU due to freshwater inputs from numerous streams, like the Peene River and Oder Lagoon. A test mussel farm was established in a shallow part in the northwestern GWB (Fig. 1) and was monitored from April 2017 until the summer of 2018 when a significant loss of mussels was observed, and no new settlement occurred. Sampling was conducted at least once a month during the main growing period (April to November).

2.1.2. Field measurements of mussel growth for the DEB model

Field data of mussel biomass, dry weight, and shell length was collected during 2017–2018 from mussel farms at the Limfjorden sites (Skive Fjord, Sallingsund, Dråby Vig) and single 100 m longlines in Mariager Fjord for calibration of the mussel growth model (Fig. 1). During 2018–2019, the same farms were sampled again in addition to 100 m single longlines deployed in new areas (Flensborg, Mariager, Roskilde, Vejle) in order to provide data for model validation (Fig. 1). Additionally, data from a pilot mussel farm located on the west coast of Latvia in the eastern Baltic Sea near Pavilosta (May to October 2018) was provided by the Baltic Blue Growth Project (Baltic Blue Growth Project, 2019) as well as GWB (Buer et al., 2020) (Fig. 1). Environmental data (temperature, salinity, chl-a) to force the model was collected from continuous monitoring stations (Limfjorden sites, As Vig, Flensborg, Mariager, Roskilde), national monitoring programs (NOVANA: Mariager, Vejle) and monthly sampling in GWB. For Latvia, we used monthly climatology from 2004 to 2018 based on available monitoring data. We then use the growth model in a farm-scale model setup at one site (Skive) to conceptually describe underlying processes influencing depletion patterns by manipulating the environmental conditions according to those representative of the study areas.

2.2. Modeling

2.2.1. Dynamic energy budget model

A process-based, dynamic energy budget (DEB) model was applied to describe mussel growth in response to temperature, salinity and food (Kooijman, 2010; van der Veer et al., 2006; Maar et al., 2009, 2015). The temperature response is a dome-shape function with highest growth at 20 °C (Maar et al., 2018). The food response follows a saturation curve except that mussel ingestion ceases at chl-a concentrations < 0.5 mg m^{-3} due to valve closure (Dolmer, 2000; Riisgård et al., 2003). The ingested food is assimilated by a constant assimilation efficiency up to 17 µg chl-a m^{-1}, whereupon the assimilation efficiency, and hence growth, is reduced exponentially due to overloading of the digestive system (Buer et al., 2020 and references therein). The model includes a salinity response to account for reduced growth at low salinities < 16 PSU (Maar et al., 2015; Buer et al., 2020). We used the most recent parameterization of the DEB model applied to German coastal waters along a salinity gradient (Buer et al., 2020). During the model calibration against field measurement from the four Danish sites for the growth period 2017–2018, only the half-saturation coefficient was changed from 0.8 µg chl-a m^{-1} to 0.7 µg chl-a m^{-1} to better match the observed growth under conditions with low food conditions. The calibrated DEB model results were validated against observations from mussel farms and test lines deployed for a growth season during 2018–2019 in different areas of Denmark, GWB and in Latvia (see previous section).

2.2.2. Farm scale setup: Skive Fjord

We used a 3D DEB farm model to evaluate the effects of environmental conditions over the spectrum of variable Baltic waters, and farm configuration on the intensity and spatial extent of chl-a depletion. The model was implemented as a decoupled setup in the FlexSem framework (Larsen et al., 2020) with baseline hydrodynamics derived from the calibrated Limfjorden FlexSem setup for 2017, while chl-a, salinity, and temperature were modified from the 2017 *in situ* time series for scenario analyses. The model mesh consisted of three zones, within a 1900x1500 m grid, the central farm area is 700x300 m made up of 25x10 m elements, surrounded by an 1100x700 m grid made up of 50x50 m

elements, and an outer grid made up of 100x100 m elements (Figure A.1); where the model 'domain' encompasses the entire mesh (all zones). Vertical resolution was 1 m, and while the model included vertical shear, no specific vertical flow or diffusion was used due to smooth bathymetry prevalent at these sites. Reference values for determining depletion ratios were derived from boundary conditions. A combination of a mask on the model grid and a mussel density function was used to couple the DEB model to the physical model. The mussel density function was created by relating individual mussel size with number per meter collector material, scaled to amount of material per unit volume. The farm scale model was validated for a 3 month (August 1–October 31) period against growth data from the Skive farm monitored over 2017, as reported in Taylor et al. (2019, Fig. 2). To describe medium-term depletion dynamics, one month-long scenarios (Table 3) included intervals of chl-a, salinity, current speeds, and the full-scale farm oriented in a perpendicular and parallel configuration (Figure A.2), where predominant currents flow along an ~185–5°axis.

The DEB was initialized for these scenarios with mussels of 2.36 cm shell length and 0.094 g dry weight. Stocking strategies were additionally tested, either fully stocked (90 lines) or partially stocked (45 lines), where lines are 200 m in length, and are situated in three sections of up to 30 lines each with sections separated by 20 m. From these scenarios, depletion patterns were quantified by relative concentrations of chl-a over the simulation to the boundary conditions (relative depletion), and spatially explicit statistics (depletion extent), described below. As temperatures between sites are not considerably different, and an energetic response to temperature is well described (i.e. Figure S4 in Holbach et al., 2020), we omitted running scenarios based on temperature manipulation. Lastly, mockups of farm setups corresponding to transects (see 2.2.1 and 2.2.2) were initialized with farm configuration, stocking, environmental conditions, and initial shell length and dry weights calculated from DEB outputs; where it should be noted that the hydrodynamics were adopted from the Skive setup described above.

2.3. In situ measurements of depletion

Periodic sampling of chl-a and Secchi depth was conducted at all depletion sites. For the Danish sites (As Vig, Limfjorden), monthly or semi-monthly samples were captured over the growing season (June-December). Water sampling was preceded by a CTD cast (EIVA Arop) to assure water mass continuity between sampling locations (Cranford, 2019). Reference positions were located 500–1000 m from each farm tangential to predominant current directions. For GWB, the farm area was small and reference positions were ~250 m from the farm. For each station, chl-a concentrations were quantified by taking triplicate water samples at 2 m depth within the farm and at the reference position, all

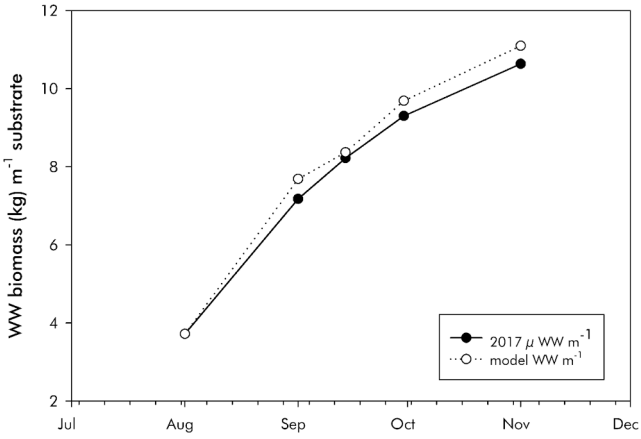

Fig. 2. Validation of farm-scale model against field data from Skive 2017, values expressed in wet weight mussel biomass per meter spat collector.

Table 3
Variables crossed for farm-scale model scenarios.

Parameter		Scenarios
O	orientation	Perpendicular, Parallel
V	Velocity (cm s^{-1})	1.27, 2.34, 4.68, 8.19, 11.7
C	chl-a (μg l^{-1})	1.8, 3.5, 5.3, 7.1, 8.9, 10.6, 12.4, 14.2
S	salinity	5.8, 11.6, 17.4, 23.2
	Stock (# lines)	45, 90

samples were filtered through 25 mm Whatman GF/F filters, filters transferred to 10 ml of 96% ethanol, covered and light-sealed, then measured for fluorescence at 665 nm before and after acidification in a Turner 10AU fluorometer (Holm-Hansen et al., 1965). Secchi depth was determined on the non-shaded side of the boat over triplicate casts.

2.3.1. Spatially discrete transects

Discrete transects measuring chl-a concentrations were conducted at As Vig, Skive, Dråby Vig, and GWB. The methodology follows procedures employed for periodic sampling, then sampling from additional points along the axes of the farm to construct spatial gradients by Inverse Distance Weighted or non-linear smoothing interpolation with the spatstat package in R (Baddeley et al., 2015), then visualizing by map contours binned over 5–10 classes by geometric intervals. In As Vig, currents were measured with a Teledyne Sentinal Workhorse 600 kHz ADCP (Acoustic Doppler Current Profiler) from ~ 10 m depth, pointing upwards, recording 1 min ensembles in 50 cm depth bins. In GWB, a Nortek Aquadopp 1 mHz ADCP was used to measure currents from 6 m depth, pointing upwards, recording every second over 4.5 cm bins.

2.3.2. Continuous transects

High resolution transects were conducted at Dråby Vig (9–2018), Skive (10–2018), and Venø Sund (8,9,10–2018; 3,4,6,7,9,10,12–2019). A Turner Cyclops 7F chl-a sensor was mounted to a bar, fixed to the side of the boat, approximately at the forefoot (bow) of the vessel, at a depth of 2 m (boat draft < 50 cm). The sensor face was oriented towards the seafloor and shaded from ambient light. The sensor position was tracked with a Garmin GPSMAP 78, and the boat traveled at speeds between 0.5 and 3 knots. Sensor readings were collated every second; 5-second averages were logged as voltage. Calibration samples were captured, extracted, and fluorometrically quantified as described above. Extracted chl-a values were then regressed against the voltage readings with a filtered seawater blank as the intercept; correlation coefficients (R^2) were consistently > 0.85. For visualization and estimation of the spatial extent of depletion, transformed values were interpolated with an empirical Bayesian kriging function over the domain of the positions with 1000 simulations using a Bayesian bootstrap method and a power semivariogram model in Python (Krivoruchko and Gribov, 2019; Gribov and Krivoruchko, 2020; Pilz and Spöck, 2008); where the power model is unbounded (Zimmerman and Stein, 2010) and provided the least residual error in these cases. This geostatistical method permits non-stationarity, accounts for measurement error, can incorporate coincident and non-regular measurements, and allows for subset spatial model definition and merging. Interpolations were bound within a convex hull delineated for each transect. Performance of the interpolations was assessed by leave-one-out cross validation of the original data. Map contours were binned by geometric intervals of the dataset over 5–10 classes for visualization. Hydrodynamics were monitored with an ADCP (Teledyne Sentinel Workhorse 600 kHz, 10 min ensembles, 50 cm depth bins) in Skive during the transects, and in Venø Sund during the 10–2018, and 6,7,9–2019 transects; otherwise a drogue at 2 m depth with surface buoy were deployed and positions noted at the beginning and ends of the transects for coarse current direction determination.

2.4. Analysis of in situ and model data

For *in situ* measurements and model outputs we calculate relative depletion as $(C_r - C_i) / C_r$, where C_r is the reference quantity and C_i is the quantity at location i; which is in the center of the farm for periodic sampling. Periodic sampling data (chl-a and Secchi depths) was analyzed by two-way PERMANOVA (1E5 permutations) in the *vegan* package in R (Oksanen et al., 2019). Normality of residuals was checked by a normal QQ plot and the Shapiro-Wilk test.

As depletion gradients are not spatially independent, we employ a spatial statistical approach to assess the extent of depletion in transects and the farm-scale model. Transect points and centroids from each element in the farm-scale model were used to construct a spatial weight matrix. Thereafter, Local Indicators of Spatial Association (LISA) were calculated with *spdep* in R (Bivand et al., 2013), following Petersen et al (2019b). Briefly, clustering of low chl-a concentrations was identified in each transect by a Moran's I statistic of $p < 0.05$, and where Getis-Ord G* values were negative. Spatial coverage of significantly low chl-a concentrations was indicated by the sum of cell areas with Moran's I statistics of $p < 0.05$ and negative Getis-Ord G* values; coverage was then converted to proportion of the study domain for each time step and scenario. To analyze the interactions of environmental conditions, hydrodynamics, and the mussel farm, relative depletion and proportional coverage of significant LISA patterns of the domain from model scenarios were evaluated with a beta regression model (Eq. (1)), using a logit link function and constant precision parameter Φ (Ferrari and Cribari-Neto, 2004). Model outputs were fully crossed and included farm orientation, ambient chl-a concentrations, salinity, and current velocity in vector X_1, and β_1 the regression coefficients calculated by Maximum Likelihood Estimation, and $\varepsilon_{depl,y}$ the error term, in the *betareg* package in R (Cribari-Neto and Zeileis, 2010). Model parsimony was accomplished by stepwise inclusion of main effects and interactions, and minimizing the Bayesian Information Criterion (BIC).

$$g\left(\mu_{depl,y}\right) = \beta_1 {}^* X_1 + \varepsilon_{depl,y} \quad (1)$$

3. Results

The updated DEB model tuned to field data exhibited robust prediction capabilities for mussel condition factors. The mockup farm-scale setups provided representative depletion signals when contrasting against *in situ* measurements, including differential biomass accumulation in response to salinity. Depletion signals from the model were most influenced by velocity, ambient chl-a concentrations, and farm orientation; where the interactions in nonlinear space could be generalized. Long-term *in situ* monitoring and transect data demonstrated that the depletion signals were variable over time and acutely related to ambient conditions and farm configuration.

3.1. Farm-scale model

3.1.1. DEB model validation

The DEB model calibration showed a significant correlation ($R^2 = 0.82$, $p < 0.001$) with monitoring data of mussel DW from four stations (Figure A.3, panel A). The model tended to underestimate the biomass in winter in Skive Fjord and Løgstør Bredning, but these stations also showed the highest standard deviations of observed biomass means (Figure A.4). The validation showed a significant correlation ($R^2 = 0.84$, $p < 0.001$) with monitoring data from 9 stations (Figure A.3, panel C). In Mariager inner Fjord, the chl-a concentrations were up to 50 μg l^{-1} and the model provided a good fit to mussel growth data. If the reduced assimilation at high chl-a concentrations was removed from the model, the shell length and tissue biomass were overestimated by the model. Calibration and validation correlation statistics are presented in Table A.2. Parameters and equations for the DEB model can be found in the supplementary material in Buer et al. (2020)[1].

3.1.2. Farm scale model

The model run against monitoring data (temperature, salinity, chl-a) and a mockup of the line configuration in Skive used in 2017 exhibited similar growth patterns to field observations, with nominally higher linear biomass loads (Fig. 2). Mean depletion rates for the 2017 Skive setup over the validation period (1. September–30. November) were on average 20.1% over the domain, and 48.4% within the farm area. Further scenario runs, based on interval modification of the environmental and hydrodynamic conditions in Skive with a full (90 lines) or half-stocked farm (45 lines) were used to derive generalized principles of depletion dynamics. As the hydrodynamic regime was only valid for Skive, further mockups representative of the other depletion monitoring sites, to contrast with *in situ* observations were performed for exploratory purposes and are detailed below with transect results (Section 3.2.2).

Mussel growth, and consequently total mussel biomass is a function of salinity and chl-a in the model. When salinity is low (i.e. < 10 PSU), there is a reduced impact on the depletion signal as mussel growth is hindered by the energetic expenditure for osmoregulation (Figs. 3 and 4). Salinities higher than 23.3 PSU (i.e. Skive salinity) were tested, but as the osmotic penalty does not take effect above 16.2 PSU (Buer et al., 2020), the results were unaffected by increasing salinity. The distribution of mussel biomass within the farm simulations was proportional to velocity, where higher velocities exhibited greater homogeneity due to increased food flux rates (Figure A.5), as well as the highest rates of biomass accumulation.

Provided spatially explicit food limitation within the center and 'downstream' parts of the farm, increased heterogeneity in mussel growth was observed with an increased relative depletion rate; where a Weibull growth relationship between the relative depletion rate [x] and interquartile range of wet weight biomass per meter collector (kg) is followed:

$$f(x) = 1.43E07\left(1 - e^{\left(-\frac{x}{2395.6}\right)^{2.2}}\right)$$

Likewise, increased depletion rates were tended to result in lower mean shell length and heterogeneity of shell length within the farm. Modeling total biomass as a nonlinear function of depletion rates, salinity, chl-a, and velocity, biomass accumulation rates diminished with increasing depletion rates, approaching an asymptote around 64% in the model domain and exceeding 90% in the center and downstream sections of the farm; an expected result of accelerating food resource limitation. Beta regression demonstrated that orientation of the farm to predominant current directions had a drastic effect on the intensity of the signal (Table 4), for example, when velocities were 1.27 cm s^{-1}, chl-a at 7.1 μg l^{-1}, salinity at 23.2 PSU, greater residence time along the axis of the farm led to an increase of relative depletion from 44.7% to 52.9%, while the coverage nominally extends from 10.1% to 10.4% of the domain (Figs. 3 and 4). Orientation is the strongest driver in the extent of the depletion signal (LISA), where a farm set perpendicular to the predominant currents exhibits greater spatial spread of the signal (Table 5, note that perpendicular is the positive value for orientation in the regression). Biomass as a function of stocking strategy also has a considerable effect on relative depletion rates (Fig. 5).

Current velocity is a significant driver of the intensity (relative depletion) and extent of the depletion signal (Tables 4 and 5). For

[1] https://www.frontiersin.org/articles/10.3389/fmars.2020.00371/full#supplementary-material

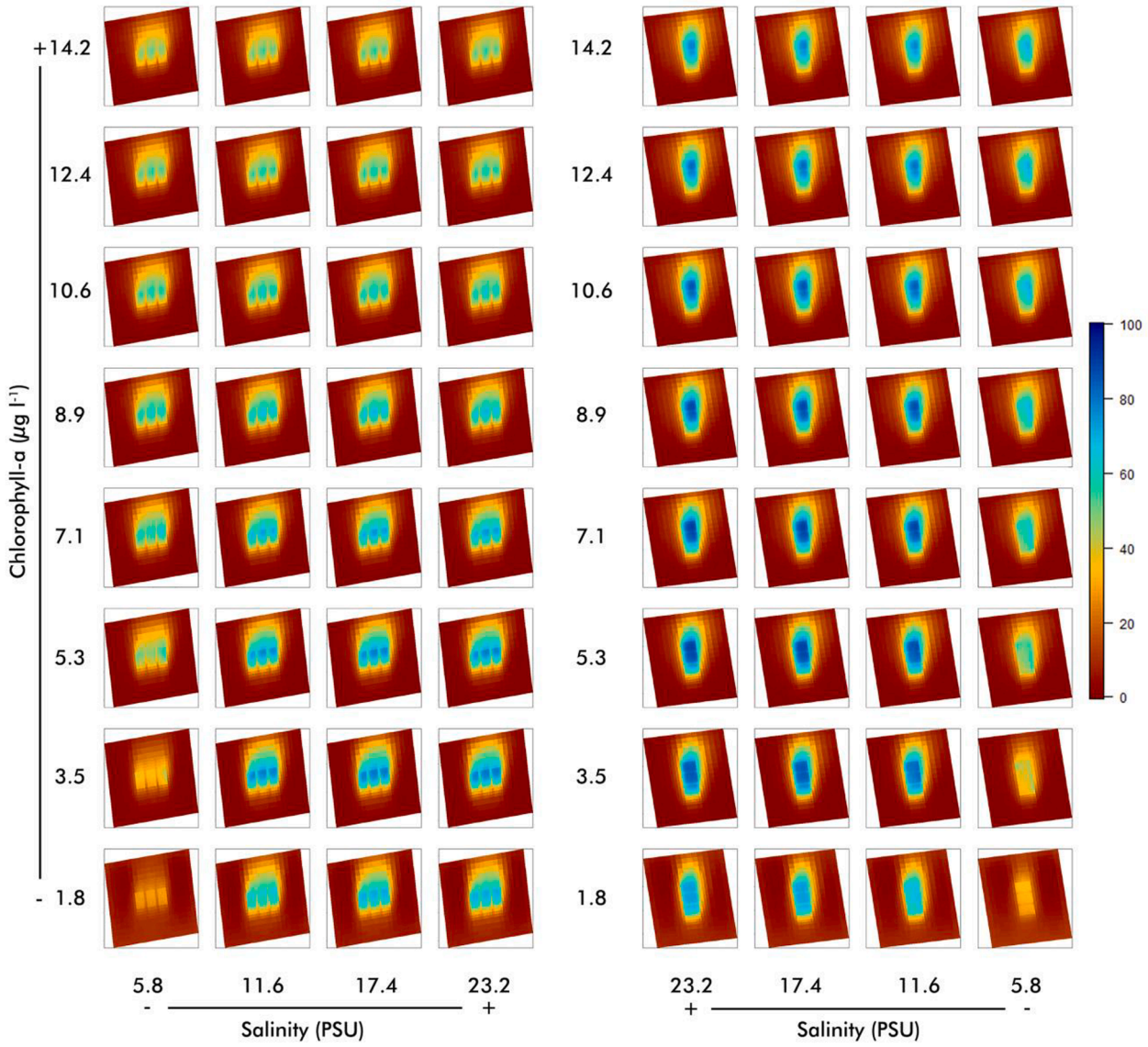

Fig. 3. Relative depletion (% difference from ambient chl-a concentrations) patterns within a fully-stocked farm (90 lies) oriented perpendicular (left) or parallel (right) to predominant currents (mean 2.6°, 1.27 cm s^{-1}). Salinity intervals increase centrally, chl-a intervals increase from the bottom to the top of the figure. Note the intensity of relative depletion is influenced by all three variables.

example, in the perpendicular orientated farm with baseline chl-a and salinity, with a moderate increase in velocity from 1.27 to 2.34 cm s^{-1} (Fig. 4), the mean relative depletion signal reduces from 44.7% to 30.2% and the extent of relative depletion (50% depletion coverage) from 10.1% to 4.6% of the domain, while clustering of significantly low concentrations (LISA) decreases from 3.7% to 2.9% of the domain. At higher velocities, such as those observed in As Vig (>6 cm s^{-1}), relative depletion rates and depletion extent are extremely diminished (Figs. 6 and 7). Increasing chl-a concentrations generally diminish the relative depletion signal in intensity and extent, due to sufficient food resources, or combined with higher current velocities (Tables 4 and 5; Figs. 3, 4, 6, and 7), sufficient flux of food, and hence, reduced relative differences in ambient food concentrations.

The highest relative depletion rates (55%) within the study domain were observed in the parallel-oriented farm, fully stocked (90 lines), median velocities of 1.27 cm s^{-1}, with full salinity (>23 PSU) and an average of 3.54 µg l^{-1} ambient chl-a. The lowest rates (1.8%) were observed at the lowest salinities (5.81 PSU), highest ambient chl-a (14.17 µg l^{-1}) and highest velocities (11.7 cm s^{-1}), in a farm only stocked by half (45 lines). Salinity, chl-a, and current velocity are positive drivers of biomass accumulation, while with increasing chl-a and velocity, salinity and biomass become less impactful on the diminishing depletion signal due to increased food flux and background concentrations (Fig. 6). Overall, biomass accumulation was highest in the scenarios run at the highest velocities, full salinity, and chl-a concentrations (Fig. 6). The lowest salinities, chl-a concentrations, and velocities, at full stock (90 lines) resulted in the lowest total biomass loads. Stocking at half (45 lines) in the lowest salinity conditions (5.81 PSU) resulted in marginally greater biomass accumulation when chl-a concentrations fell below 5.31 µg l^{-1}, yet the depletion rates are still higher when fully stocked; for example, at a median salinity of 5.81 PSU and ambient chl-a concentration of 5.31 µg l^{-1} in a farm aligned perpendicular to the currents, half stocked (45 lines) provides 175 t of mussels and a mean relative depletion rate of 35.9%, while a fully stocked farm (90 lines) provides 156 t of mussels and a 37.3% relative depletion rate.

Non-linear interactions in regards to relative depletion and extent (Fig. 7) were observed between chl-a concentrations, farm biomass, and current velocities. In both cases, the depletion signal responds rapidly to reducing current velocities, increasing biomass, and reducing chl-a concentrations.

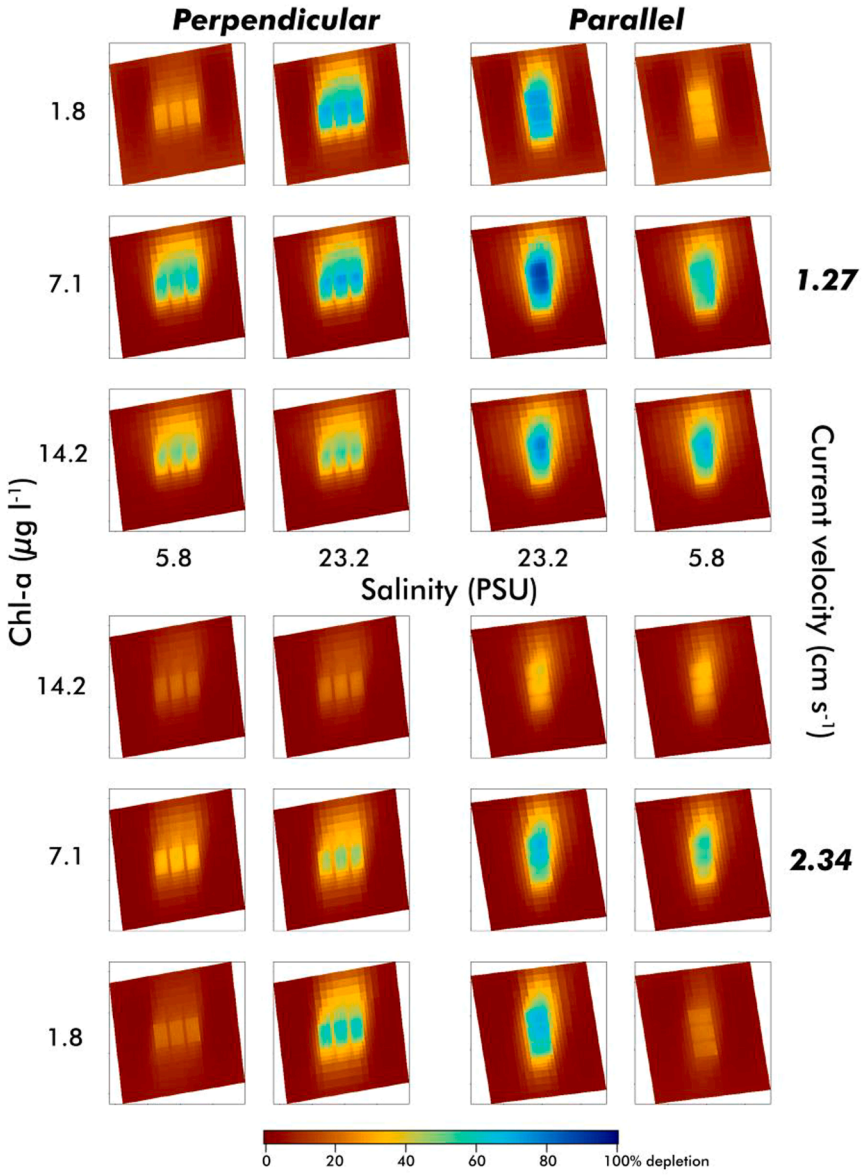

Fig. 4. Relative depletion (% difference from ambient chl-a concentrations) patterns within a fully-stocked farm (90 lies) oriented perpendicular (left) or parallel (right) to predominant currents at baseline velocities (1.27 cm s^{-1}) and moderately increased velocities (2.34 cm s^{-1}). Salinity and chl-a intervals increase centrally.

Table 4
Beta regression model on relative depletion (mean chl-a in the farm / mean chl-a at the boundary). C = chl-a, O = orientation, S = salinity, V = velocity, ϕ = precision parameter, ~R^2 = pseudo R^2. Confidence interval of coefficients are presented at 5% and 95%.

Parameter	Estimate	Std Error	X^2	p value	5%	95%
V	−0.255	0.014	340.227	<0.0001	−0.283	−0.228
C	−0.076	0.007	108.228	<0.0001	−0.090	−0.061
O	−1.283	0.181	50.059	<0.0001	−1.638	−0.928
O*V	−0.452	0.076	35.439	<0.0001	−0.600	−0.303
S	0.016	0.004	19.010	<0.0001	0.009	0.023
C*V	−0.013	0.003	18.335	<0.0001	−0.018	−0.007
C*S	−0.003	0.001	9.457	0.002	−0.004	−0.001
ϕ	0.028	0.002	193.86	<0.0001	0.024	0.032
~R2 = 0.872						
Log likelihood = 350.164						
BIC = −650.35						

3.2. *In situ measurements of depletion*

3.2.1. *Periodic sampling*

Between 2017 and 2018, differences in chl-a and Secchi depth were tracked for Skive, Dråby Vig, and Sallingsund, while Venø Sund was monitored over 2018–2019. Throughout the growing and monitoring season, stratification (Δ salinity, temperature 50 cm^{-1} > 0.5 PSU, 1 °C) was generally observed 3.5–4.0 m below the sea surface, and water column profiles were similar between the farm area and reference stations with the occasional exception of Venø Sund, of which the northern extent of the farm was more saline (e.g. 30.5 PSU) than the southern reference point (29.5 PSU) that were located ~ 3.5 km apart. Reduction in chl-a concentrations over the growing season within the farm ranged between 8 and 42% in Dråby Vig, 13–36% in Sallingsund, 7–42% in Skive, and 6–69% in Venø Sund (Fig. 8). Secchi depth improvement ranged between 0.35 and 1.5 m in Dråby Vig (10–50%), 0.4–1 m in Sallingsund (20–50%), 0.35–1.25 m in Skive (9–50%), and 0.1–1.85 m in Venø Sund (0–67%, Fig. 8). These trends tended to follow biomass accretion to the maximum relative differences approximating harvest timing (autumn, Table 1). As Vig, as a site more representative of open

Table 5
Beta regression model on % area with significant (LISA) depletion patterns. C = chl-a, O = orientation, S = salinity, V = velocity, ϕ = precision parameter, ~R^2 = pseudo R^2. Confidence interval of coefficients are presented at 5% and 95%.

Parameter	Estimate	Std Error	X^2	p value	5%	95%
O	0.593	0.019	936.553	<0.0001	0.555	0.631
V	−0.032	0.001	659.344	<0.0001	−0.034	−0.029
O*V	0.127	0.009	203.570	<0.0001	0.109	0.144
C	0.016	0.001	127.840	<0.0001	0.013	0.019
C*V	−2.16E-03	3.28E-04	43.303	<0.0001	−0.003	−0.002
C*O	−0.006	0.002	7.137	0.008	−0.010	−0.002
ϕ	4.87E-04	4.80E-05	102.6593	<0.0001	3.92E-04	5.81E-04
~R2 = 0.942						
Log likelihood = 864.1						
BIC = −1683.776						

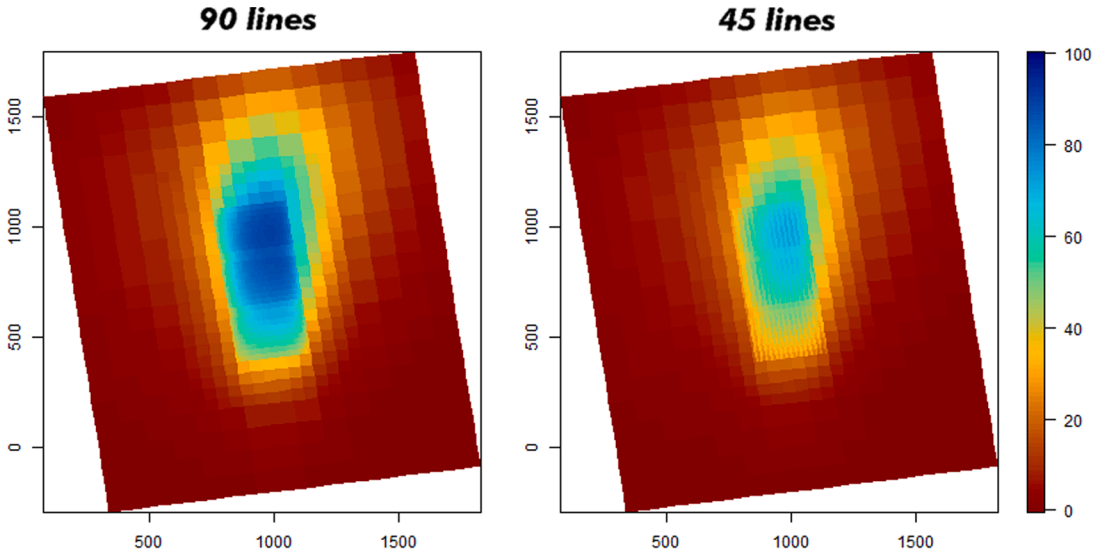

Fig. 5. Relative depletion (% difference from ambient chl-a concentrations) patterns between a fully-stocked and partially-stocked farm under identical environmental conditions. mean velocities = 1.27 cm s^{-1}, salinity = 23.2 PSU, chl-a = 7.1 μg l^{-1}.

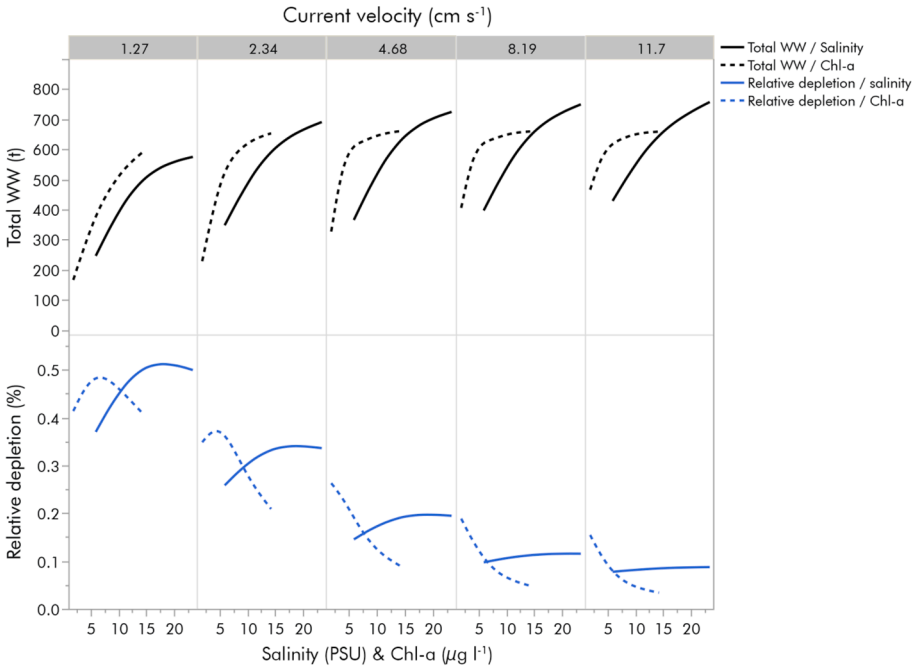

Fig. 6. Effect of salinity (PSU) and chl-a (μg l^{-1}) on biomass (total WW - top) and the relative depletion signal (bottom) over different current velocities (cm s^{-1}). Salinity curves are represented as solid lines, chl-a as dashed lines.

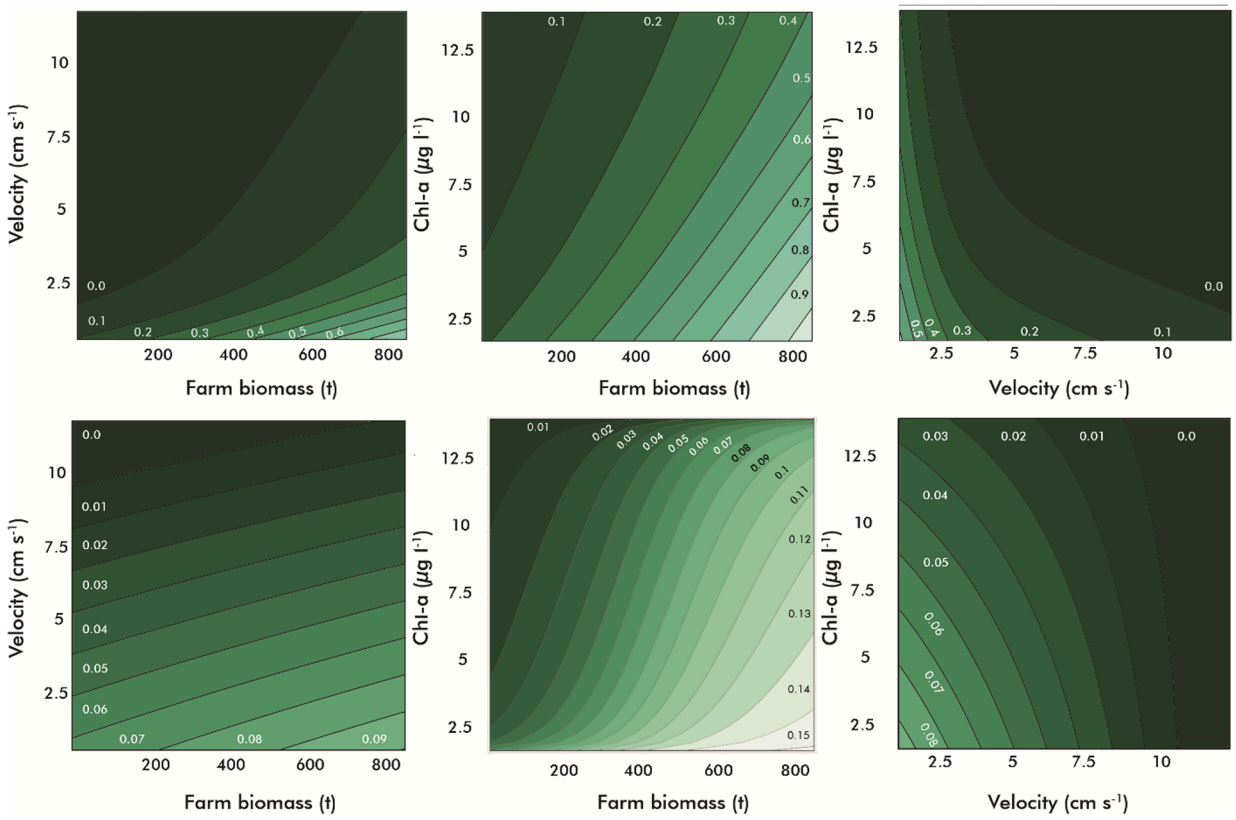

Fig. 7. Contour plots of relative depletion (top panels) and depletion coverage (% area of the domain with > 50% depletion, bottom panels) by total biomass in the farm (t), ambient chl-a concentrations (µg l^{-1}), and current velocity (cm s^{-1}). Due to the non-linear effects on relative depletion, contours constructed by fitting a hyperbolic tangent function over all linear combinations of parameters using mean values over each model run for the parallel orientation section setup (top. R2 = 0.98, RMSE = 0.026; bottom. R2 = 0.94, RMSE = 0.01). Relative depletion and depletion coverage values are indicated within the plots. Salinity is constant at 23.5 PSU, in the left plots chl-a is constant at 7.1 µg l^{-1}, in the center plots velocity is constant at 1.27 cm s^{-1}, and in the right plots biomass is constant at 500 t.

Kattegat waters, has higher current velocities and deeper waters than the typical farm site in the Limfjorden, with lower chl-a concentrations (Table 2). Over the monitoring period, reduction of chl-a ranged between 0 and 27% (Fig. 8), while Secchi depth improvements ranged between 0.5 and 2.25 m (10–50%, Fig. 8), with increasing trends to the autumn prior to harvest in October 2018. Conditions in GWB differ considerably from the other sites, provided considerably higher ambient chl-a concentrations and low salinity (Table 2). Between October 2017 and July 2018, prior to loss of mussel biomass (July 2018), relative chl-a depletion rates between −14 and 33% were observed (Fig. 8), with no clear association with biomass accumulation or chl-a concentrations; in two sampling events, chl-a concentrations were higher within the farm. Over all sites, chl-a concentrations were significantly lower ($F_{1,110}$ = 4.97, MSS = 33.748, p = 0.0198) and Secchi depths significantly greater ($F_{1,92}$ = 16.38, MSS = 18.567, p < 0.001) within the farm areas than the reference position. Regressing relative depletion of chl-a against relative Secchi depth improvements provided poor correlation over all sites and sampling events (R^2 = 0.067, RMSE = 0.166, p = 0.072).

3.2.2. *Chl-a transects*

Dråby Vig: A single transect was performed on 14-9-2018 in Dråby Vig, in the northern half of the farm area, where depletion rates within the farm were on average 46%, when biomass within this farm section was estimated to be 98 t (4.2 t ha^{-1}) and ambient chl-a concentrations of 1.67 µg l^{-1}, and current directions oriented toward 15°. Significant clustering of low chl-a concentrations was found in the center of the farm and immediately northeast of the farm, while high concentrations were focused several hundred meters northwest of the farm. The farm-model scenario corresponding to conditions representative of the site (perpendicular, current velocities = 1.27 cm s^{-1}, chl-a = 3.54 µg l^{-1}, salinity = 23.23 PSU) exhibited total biomass yields of 497 t and a mean relative depletion rate of 41% and 69% in the center of the farm. Running the model for the configuration used at the site at that time (26 lines), total biomass yields were 103 t, with a mean relative depletion rate of 14% and a maximum of 54% in the farm.

Venø Sund: Depletion within the Venø Sund farm ranged between 27% and 69%, while the intensity of depletion was associated with ambient chl-a concentrations, an increasing signal was observed to propagate towards the northern sections of the farm area, following predominant current directions. Two transects from June and July of 2019 are presented in Fig. 9. Spatial estimates of the geostatistical model suggest an extent of the depletion signal of several hundred meters around the farm area, which was often observed west and north of the farm. Clustering (LISA) of low concentrations was consistently found within the farm area, while high values were typically at the south-eastern and northeastern extents of the transect domain. The farm-model scenario corresponding to conditions representative of the site (parallel, current velocities = 2.34 cm s^{-1}, chl-a = 5.31 µg l^{-1}, salinity = 23.23 PSU) exhibited total biomass yields of 720 t and a mean relative depletion rate of 31% and 55% in the farm.

Skive Fjord: Two transects performed at Skive in the center and east of the farm (29,31-10-2018) presented relative depletion rates within the farm area between 11 and 45%, their merged interpolations are presented in Fig. 10. Low chl-a concentrations were clustered (LISA) within the core of the farm, while high values were found immediately east of the farm. A discrete transect performed in Skive on 13-9-2017 with seven locations, 5 outside, 2 inside of the farm, exhibited an average of 49% depletion within the farm, 28% north, 23% west of the farm with decreasing rates south and east of the farm, where it was noted currents were directed north, biomass estimated to be 477 t (21.8

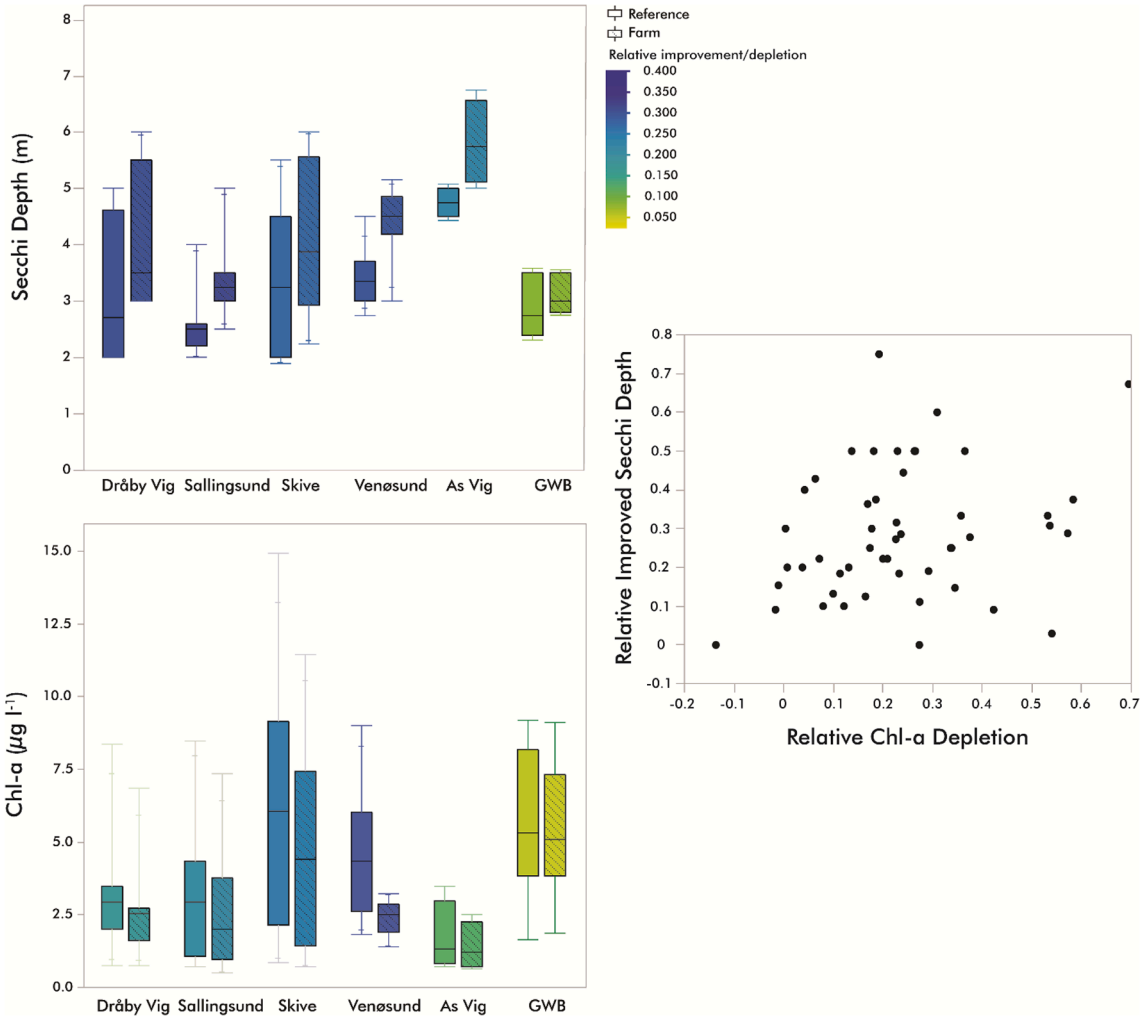

Fig. 8. Relative Secchi depth improvement and relative depletion of chl-a between reference positions and the farm over the monitoring period. Colors indicate degree of relative difference, box plots represent measured Secchi depth (m) and chl-a (µg l^{-1}) values. The scatterplot on the right presents simultaneous measured relative differences of chl-a (x-axis) and Secchi depth (y-axis) over all sites; note the weak positive association.

t ha^{-1}), and ambient chl-a concentrations of 5.59 µg l^{-1}. The farm-model run on the same configuration as the 2017 setup exhibited total biomass yields of 521 t and a mean relative depletion rate of 31% and 44% in the farm.

As Vig: A discrete transect was conducted in As Vig on 26-10-2018 with 1 point at a reference position northwest of the farm, 2 points at the northern and southern corners of the farm, and one in the center of the northern section of the farm (Figure A.6). A depletion gradient was observed within the farm and south of the farm following currents (305.8°), however, the extent of this pattern is uncertain due to limited spatial representation; LISA statistics indicated dispersal, with significant low concentrations within the farm and high in the northern points. The overall observed relative depletion rate was 16% and 27% in the center of the farm, while mean current velocities were 7.15 cm s^{-1}, chl-a concentrations 29.1 µg l^{-1}, and total biomass of 729 t (64.5 t ha^{-1}). The farm-model scenario corresponding to conditions representative of the site (parallel, current velocities = 8.19 cm s^{-1}, chl-a = 3.54 µg l^{-1}, salinity = 23.23 PSU) exhibited total biomass yields of 716 t (729 ± 24.7 t measured in the field) and a mean relative depletion rate of 15% and 26% in the center of the farm.

GWB: In the discrete transect (14-6-2018), the center of the farm exhibited 10.8% depletion, while 'downstream' of the farm was 13.5% using the eastern measurements as reference, while currents were predominantly flowing from the east to west (median 85.95°) at 2.16 cm s^{-1} during the sampling period. A depletion gradient is visible in Figure A.7 approximating the current direction, however, LISA statistics indicate no clustering of low or high values. The fully stocked farm-model scenario corresponding to conditions representative of the site (parallel, current velocities = 1.27 cm s^{-1}, chl-a = 12.4 µg l^{-1}, salinity = 5.81 PSU) exhibited total biomass yields at 406 t and a mean relative depletion rate of 40% and a maximum of 72% in the farm. Running the model for the configuration used at the site (5 lines × 50 m), total biomass yields were 2.5 t (2 t measured in the field), with a mean relative depletion rate of 3% and a maximum of 8% in the farm.

4. Discussion

4.1. Mechanisms resolving extent and intensity of depletion signal

Over the scenario farm-scale model runs, it was clear that moderate changes in current velocity (Figs. 5–7) and the interaction with chl-a concentrations markedly influenced the intensity and extent of the depletion signal, while farm orientation had less effect (Tables 4 and 5, Figs. 3 and 4). The farm-scale model is essentially a dispersed plug-flow reactor design. Orienting the farm perpendicular to currents reduces the retention time of a water mass parcel within the area of active filtration. This permits greater overall exposure of the cultivation unit to relatively higher food concentrations, but limits the local intensity (relative

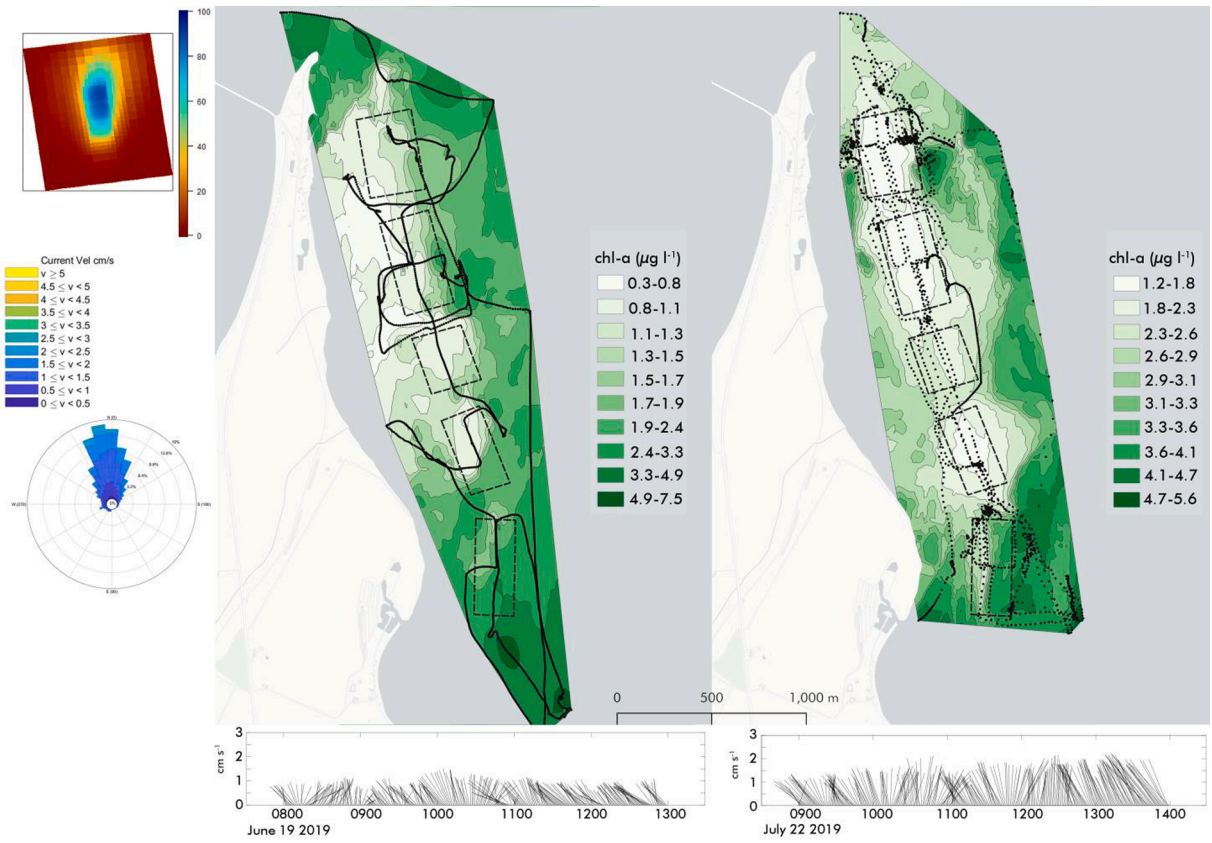

Fig. 9. Bayesian kriging interpolation (Gribov and Krivoruchko, 2020) of continuous chl-a transects at the Venø Sund farm. Chl-a isolines were drawn on 10 bins determined by geometric interval over each respective distribution, transect paths are presented as dots, and the interpolation bound by a convex hull. **Left**. June 19, 2019, mean current velocity = 1.17 cm s^{-1}, estimated farm biomass = 1980 t (26.8 t ha^{-1}), mean chl-a = 1.74 μg l^{-1}, relative farm depletion = 0.69, relative domain depletion = 0.59; cross validation. $R^2 = 0.94$, RMSE = 0.088, $F_{1,3425} = 51967.04$, $p < 0.001$. **Right**. July 22, 2019, mean current velocity = 1.65 cm s^{-1}, estimated farm biomass = 2400 t (32.4 t ha^{-1}), mean chl-a = 3.29 μg l^{-1}, relative farm depletion = 0.56, relative domain depletion = 0.32; cross validation: $R^2 = 0.93$ RMSE = 0.192, $F_{1,1620} = 23736.9$, $p < 0.001$. The farm areas are dashed rectangles. Mean current speed and direction over the water column at plotted over the transect time period below respective transects in quiver plots. A farm-model setup, visualizing mean relative depletion patterns over September, corresponding to environmental conditions representative of the site (mean velocity = 1.27 cm s^{-1}, chl-a = 5.31 μg l^{-1}, salinity = 23.23 PSU) is presented in the top left. Predominant currents are presented in a rose diagram at the center left.

depletion) of water clarification (Fig. 5). Nevertheless, given the same area, depletion intensity is spread to a greater area (note a positive coefficient for orientation in Table 5). From a production and nutrient accumulation perspective, food limitation is undesirable when heterogeneous growth (bulk mass) leads to overall reduced biomass yields (Friedland et al., 2019a; Taylor et al., 2019). From a mitigation perspective, where heterogeneity in mussel size is not a quality factor, the local effect is similar to placing multiple perpendicular farms in series along the predominant current axis. Previous investigations have found inverse linear relationships with current velocities and the intensity of the depletion signal, noting the importance of residence time within the cultivation units related to orientation (Cranford et al., 2014; Newell and Richardson, 2014; Nielsen et al., 2016; Petersen et al., 2019b); while other studies could not find a correlation (Petersen et al., 2008). In microtidal environments with lower current velocities (<4cm s^{-1}), which are prevalent in Baltic coastal waters, these findings suggest prioritizing perpendicular orientation for mitigation farms will yield higher biomass (nutrient extraction) and greater spread of the depletion signal over the larger water body. High wind or current exposure and increased loading on the aquaculture structure in a perpendicular orientation can result in loss of biomass and damage to the farm.

As Newell et al. (2019) illustrates, resolving farm-scale hydrodynamics is critical for accurately describing depletion patterns and intensity. An important aspect of farm orientation or configuration is hydraulic drag and subsequent hydrodynamic implications (Plew, 2011; Cranford et al., 2014; Tseung et al., 2016), of which we do not resolve in the model. We use an open source 3D framework (FlexSem) with straightforward capabilities of integrating biophysical and biogeochemical sub models, but without field measurements of drag coefficients, so we must assume that depletion will be enhanced with increased structural density. Several model studies have demonstrated that reduced flow within the farm will enhance food depletion within the core of the farm (Rosland et al., 2011; Cranford et al., 2014; Newell and Richardson, 2014), and further exacerbating heterogeneous growth gradients as our model has described. Spacing between lines is a critical factor to describe the effect of integrated farm hydraulic drag. Rosland et al. (2011) describe nominal impacts on depletion above 10 m spacing; whereas the farms and the farm-scale model investigated in this study implement an 8–40 m spacing between longlines or tube-nets. Increased velocities will result in greater turbulence within the canopy, which will in turn increase velocities around the farm while decreasing within the farm, and further enhance entrainment in the vertical field (Stevens and Petersen, 2011; Stevens and Plew, 2019). Normal or tangential orientation of the suspended canopy elements (i.e. the continuous loops or other substrate configuration) to the flow direction will dramatically influence the distribution of food within the canopy (Newell and Richardson, 2014), as well as the physical forces on the farm structure.

Re-filtration is often not considered in modeling simulations and is important from the coarse provision of suitable food to the mussels, and more specifically, to the modified size distribution of food within the

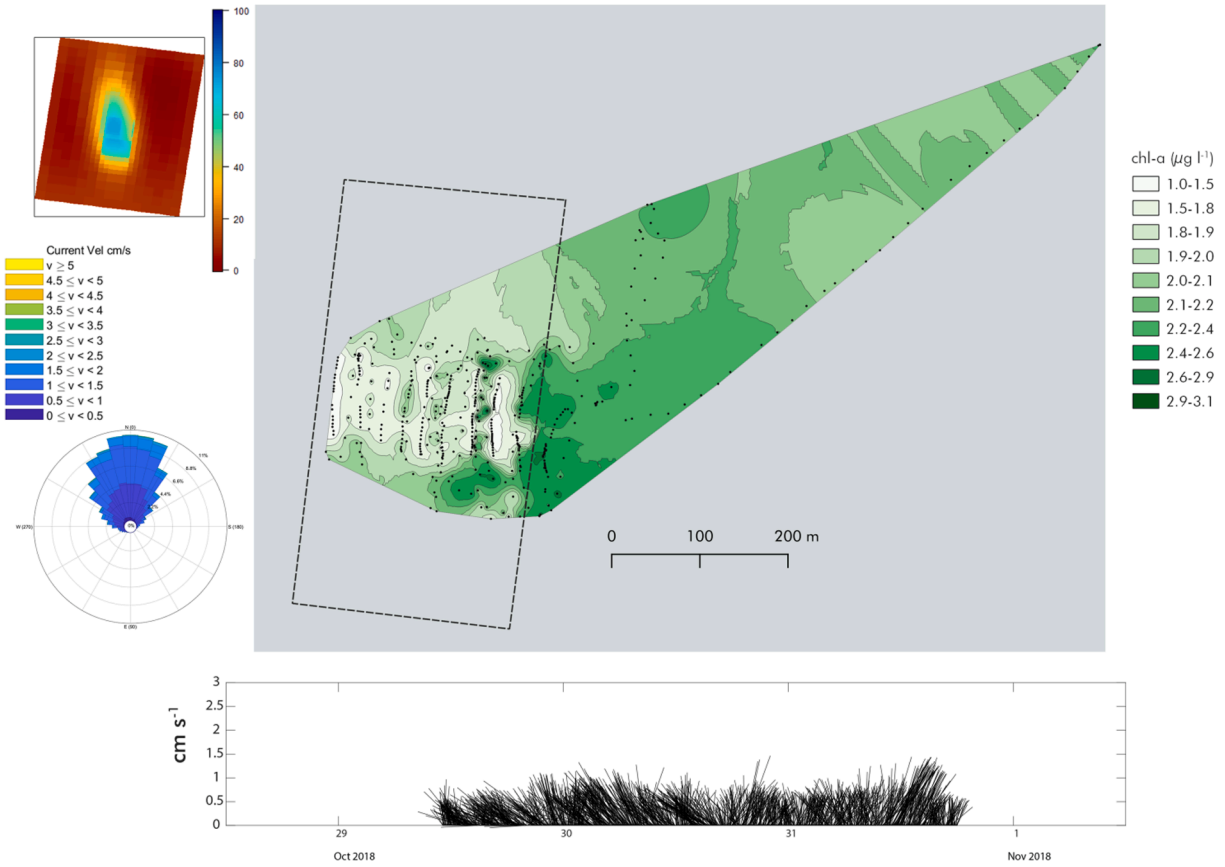

Fig. 10. Bayesian kriging interpolation (Gribov and Krivoruchko, 2020) of continuous chl-a transects at the Skive farm between October 29–31 2018. Chl-a isolines were drawn on 10 bins determined by geometric interval. Median current velocity = 0.79 cm s^{-1}, estimated farm biomass = 507 t (23.2 t ha^{-1}), mean chl-a = 1.92 µg l^{-1}, relative farm depletion = 0.33, relative domain depletion = 0.11; cross validation: R^2 = 0.65, RMSE = 0.151, $F_{1,475}$ = 886.3, $p < 0.001$. The farm area is a dashed rectangle. Current speed and direction over the water column are plotted over the transect time period below the transect interpolation in a quiver plot. A farm-model setup, visualizing mean relative depletion patterns over September, corresponding to environmental conditions representative of the site (man velocity = 1.27 cm s^{-1}, chl-a = 5.31 µg l^{-1}, salinity = 23.23 PSU) is presented in the top left. Predominant currents are presented in a rose diagram at the center left.

water mass parcel with diminishing potential capture efficiency (Cranford, 2019). The present modeling exercise addresses re-filtration from a linear form following current vector fields, discretized by mesh cell, by treating chl-a as a 100% efficiently filtered food source. The DEB model has been developed with chl-a field data, and assumes a 'built-in' effective size distribution and pool of nutritional constituents; i.e. while a portion of the chl-a pool may not be filtered efficiently or with varying nutritional content, the remaining fraction parameterizes chl-a as food and this ratio is assumed to be constant. The model also does not include a resuspension feature, which is periodic in these sites and may significantly alter the quality of seston available as food. Nevertheless, resuspension typically impacts the lowest 2–3 m at these sites, the vertical extent of the farm structure has been recommended to be maintained within the upper 3 m for optimal food quality (Filgueira et al., 2018) and optimal maintenance of the mussel aggregates (Taylor et al., 2019).

The model moderately overestimated biomass accumulation (Fig. 2) and while average depletion rates over month-long scenarios cannot be directly compared with transects, depletion rates tended to match within the study domain. In GWB, where mussel biomass was very low due to low salinity, and chl-a concentrations tended to be high (Tables 1 and 2), a minimal depletion signal was present (Figures 8 and A.7). The model demonstrates that low salinity and elevated chl-a concentrations (Fig. 3) at full stocking exhibits low depletion signals, and will be even more reduced with reduced stocking density (Figs. 6 and 7). The relationship of salinity to depletion is indirect, as filtration rates are not necessarily reduced by low salinity, rather the reduced somatic growth rates at low salinities yield lower total biomass relative to higher salinity conditions (Maar et al., 2015; Buer et al., 2020). While a limited number of farm-scale models have previously investigated differential biomass accretion with an underlying DEB model (Guyondet et al., 2010; Rosland et al., 2011), gradations of salinity as a driver of discrete biomass growth and subsequent depletion signals combined with configuration scenarios and seston loads has been seldom investigated. This is an important component to consider for implementation of mitigation mussel farms in the greater Baltic Sea.

In general, the farm-scale model tended to exhibit maximum depletion rates in conditions similar to those experienced in the Limfjorden sites, which consistently exhibited higher depletion rates than As Vig and GWB. As such, the model served as a useful tool to demonstrate that moderate changes in chl-a concentrations and velocity will drive variability in the intensity and extent of the depletion signal; in which at most sites we observed there to be a great deal of seasonal or shorter-term variability (Fig. 8). Spatiotemporal variability in seston concentrations, contents, and hydrodynamics at the farm interface can confound the quantification of depletion, which generally requires higher resolution in the monitoring program (Cranford et al., 2014). Observed depletion patterns from continuous transects were often hyper-localized around the mussel cultivation structures (e.g. Fig. 10), while higher biomass loads tended to produce widespread depletion patterns (e.g. Fig. 9). The model resolution, while fine within the farm, was still coarser than the transect resolution, as such, patterns tended to appear more continuous and diffuse. In terms of eutrophication mitigation services, balancing biomass maximization (i.e. nutrient

extraction) and seston depletion (water clarification) will require consideration of farm configuration relative to the local conditions, where in very general terms, we observed an optimization point at approximately 64% depletion within the model domain. Cranford and authors (2014) likewise observed a maximum depletion point at 56% in Spanish rafts in a macrotidal environment as a result of refiltration. Exceeding the optimization or maximum depletion level may result in stunted growth in heavily depleted sections of the farm, which will become exacerbated as mussels at the periphery of the farm continue to grow, and reduce the overall mitigation effect. Therefore, in regions or at sites with relatively coarse data resolution, the model can serve to provide managers with estimates on expected production and scale of depletion for configuring mitigation farms.

4.2. Resolution of different methods

Secchi depth and chl-a can often be covariant, however, each are quantifying fundamentally different properties in both content and dimension. As an integrated measure of water transparency, Secchi depth is a simple metric describing light scattering and attenuation over depth that is a product of distributed particle loads (scattering and absorption) and colored dissolved organic matter (CDOM; absorption (Kirk, 2011)); of which the inherent properties are unknown. Phytoplankton concentrations are primarily quantified by chl-a, and is a point measurement in both horizontal and vertical planes, but still represents particles without information of their optical properties. The two metrics are often inversely correlated (reduced chl-a concentrations, increased Secchi depth) but the direct relationship between the two is not definitive (Harvey et al., 2019), provided variable suspended matter concentrations and constitution in different water bodies (Lind, 1986); as such, it has repeatedly been suggested that such metrics (integrated and optical) are complementary (Fleming-Lehtinen and Laamanen, 2012). The poor correlation found here between chl-a and Secchi depth improvements (Fig. 8) echoes this requirement for complementary indicators for characterizing eutrophic conditions. The effect of mussel filtration on water transparency, and thereby Secchi depth, depends on the absorbing and scattering constituents of the water column, where particles (phytoplankton, particulate organic matter, larger tripton) are immobilized, while CDOM is generally unaffected. In basins with elevated concentrations of either autochthonous or allochthones CDOM, the depletion effect may not significantly influence Secchi depth, and the influence of bivalve grazing on concentration modifications of degradative humic compound byproducts has not been studied. We see here a consistent concomitant reduction in chl-a and increasing Secchi depth within farms relative to outside of the farms under study (Fig. 8), even though their relative improvements were poorly correlated. In general, there is often high variability in the correlation between total suspended matter (partially represented by Secchi depth) and chl-a depletion due to mussel filtration size-selectivity, and in productive systems, chl-a is a more reliable metric of filtration-induced concentration reduction (Cranford et al., 2014). Furthermore, as Secchi depth integrates numerous components that are modified unequally through mussel filtration, the combined discrete (spatially) sampling nature and integrated components impacting light attenuation are far less accurate than continuous measurements of single components (i.e. chl-a, particle characterization). Recent modeling efforts have described increases in Secchi depth 200 m around a mussel farm, however, this assumes phytoplankton constitutes the majority of the seston, and in such cases, the two indicators describe the same process (von Thenen et al., 2020). We observed here from *in situ* (Figs. 8–10, A.6 and A.7) and modeling that chl-a depletion can be detected hundreds of meters around farms (Figs. 3–5), increasingly so with biomass loads (Figs. 5–7 and 9). As phytoplankton (measured as chl-a) constitute a major proportion of the seston mass in mesotrophic and eutrophic waters, this depletion measure will consistently represent water clarification in eutrophic waters where Secchi depth is substantially influenced by suspended matter.

The model employed here assumes homogeneous boundary conditions at each time step, which as seen in the continuous transects, deviates from reality (Figs. 9 and 10). As such, depletion patterns will additionally be modified by the heterogeneous horizontal and vertical concentration gradients entering the farm. Spatial heterogeneity and gradation of seston concentrations and quality (chl-a, organic matter, etc.) are central features of marine, and in particular, estuarine waters, having long been recognized in the horizontal, vertical, and temporal dimensions (Fegley et al., 1992). Depletion may be confused with natural variability in cases with lower biomass (Fig. 7, A.7) (Schröder et al., 2014), high ambient chl-a concentrations (Figs. 3, 4, 6, 7, and A.7), or higher current velocities (Figs. 4, 6, 7, and A.6). In the case of As Vig and GWB, an apparent depletion signal is detected following the direction of the currents over the measurement period (Figures A.6 and A.7 respectively), however, multiple measurements over several days and optimally under a variety of conditions is needed to quantify the interactions of physical processes and mussel filtration. High resolution synoptic surveys can reveal small-scale variability in chl-a spatial distribution, which can be helpful in resolving interactions between the farm structure (canopy) and the biophysical regime (Cranford, 2019). Using a towed undulating apparatus, volumetric-based depletion rates were earlier measured at the Skive site by Nielsen et al. (2016), where 13–31% depletion rates were observed. Our transect approach used a fixed depth (2 m) which assumes an average concentration along a vertical gradient and subsequent average depletion rate in the farm of 33%.

In practical terms, continuous transects are very time consuming and susceptible to errors related to patchiness and advection. Discrete transects provide a much coarser, yet similar overall depletion pattern (i.e. relative difference), but are hindered to a greater degree by potential error due to patchiness and variable hydrodynamics (Figures A.6 and A.7) (Jansen et al., 2016). Discrete (point) transects present a snapshot of a water mass in time, with very low capability to describe depletion patterns and tend to provide very high variability, while continuous transects tend to capture medium-term variability and can simultaneously describe depletion patterns and the distribution of variability over the transect domain. Interpolations assume the concentrations at those positions are constant, and the prediction error tends to increase with the distance between points (Holbach et al., 2013). In a dynamic environment with non-stationary values, it can be difficult to interpret transect data, however, the empirical Bayesian kriging model provides a means to deal with non-stationarity (kernel convolution) and quantify uncertainty, with greater accuracy of spatial distributions of chl-a in a dynamic medium (Figs. 9 and 10). Combined with farm-scale model scenarios, transects and geostatistical modeling can help resolve and optimize farm configuration for maximizing the impacts of mussel mitigation culture.

4.3. Ecological implications and management

The direct effect of mussel farms on chl-a concentrations and Secchi depth imply significant immobilization of organic matter in eutrophic waters – a primary goal of water quality improvement programs. In terms of water quality management and the concerted use of mussel farms for improving these indicators, local conditions and priorities will determine if depletion intensity, extent, or overall immobilization of organic matter are optimization points. As a proxy for suspended organic matter, mussel biomass accumulation is the most direct measure of basin-scale reduction of organic matter when growth is not hindered by salinity stress. On the basin scale, it should be expected that organic particle depletion will be proportional to total biomass yield. From an ecosystem-scale perspective, leveraging mussel filtration for basin-scale water clarity requires an evaluation of import and export mechanisms of organic matter. Coupling farm-scale models to basin-scale ecological models could facilitate management of chl-a as an ecological indicator (Ferreira et al., 2008); where long time series and ecosystem modeling

are required to evaluate basin-scale impacts (Timmermann et al., 2019). Considering the multiple feedbacks (nutrient regeneration) and reorganization of organic matter transport through the ecosystem from large-scale mussel cultivation, and the high variability in depletion dynamics, the degree of basin-scale depletion from individual farms requires further investigation.

If mitigation mussel culture, alone or combined with terrestrial measures, achieves improved ecological conditions of estuarine and coastal systems, mussel biomass accumulation will become self-limiting; particularly in basins with low retention times (Strohmeier et al., 2008; Filgueira et al., 2015). In the case of mitigation culture, a production carrying capacity approach is used, as the purpose is to maximize organic particle immobilization and nutrient assimilation (Taylor et al., 2019); improved trophic regimes will require adoption of approaches integrating broader ecosystem interactions (Grant and Pastres, 2019; Smaal and van Duren, 2019; Weitzman and Filgueira, 2020). As either persistent top-down filtration pressure, modified nutrient flows, or climate change impact the concentration and composition of estuarine planktonic constituents (Winder et al., 2017), updating the DEB model to accommodate specific constituents and the use of community indicators can improve the understanding of ecosystem responses (Garmendia et al., 2013; Ní Longphuirt et al., 2019).

5. Conclusion

The implementation of mitigation mussel culture around the Baltic Sea will require production and impact planning at multiple scales. Concerning the impacts on two fundamental ecological indicators, chl-a and Secchi depth, the depletion of suspended particles by mussel filtration in suspended culture will be a function of farm configuration and interactions of ambient environmental conditions. The current study evaluates several of these interactions and mussel farm configurations in relation to intensity and spatial extent of particle depletion for a generalized understanding of depletion dynamics over varying conditions. Model simulations demonstrated that the intensity of the depletion signal was most dependent on current velocities, chl-a concentrations, salinity (i.e. biomass regulator) and the orientation of the farm; which related to food flux and when exceeding ~ 64% in the model domain, negatively impacted total biomass in the farm. The spatial extent of the depletion signal was exacerbated by reorienting the farm perpendicular to predominant currents, which also permitted higher biomass accumulation, and by association higher nutrient extractive capacity; although in practice, this may jeopardize structural integrity and increase maintenance costs under increased loading. Importantly, with the salinity response included in the DEB model, the integrated model was able to demonstrate reduced biomass accumulation and subsequently reduced depletion signals in lower saline waters. Field observations over sites with markedly different ambient conditions and farm setups were scrutinized to evaluate how these predictions matched with reality. A great deal of variability in depletion was observed in the field over several months and between sites, illustrating that depletion in extent and intensity is truly as dynamic as the environmental conditions between these sites. Nevertheless, variation in the signal was reflected by general nonlinear relationships predicted by the model. As much of the prior work on evaluating depletion has been conducted in limited spatial and temporal contexts, the present findings may supplement current knowledge for planning and management purposes. The potential for synergistically leveraging mussel cultivation for water clarification and nutrient binding for ecological restoration of eutrophic coastal waters could benefit from strategic design criteria to best suit a farm and farming strategies to the local environment.

Funding

This study was conducted under the MuMiPro project (Mussel farming, mitigation, and protein source for organic husbandry) project, 6150-00008B, funded by the Danish Innovation Fund, and the BONUS OPTIMUS project (Optimization of mussel mitigation cultures for fish feed in the Baltic Sea) as part of the, funded by the BONUS program (Baltic Organizations' Network for Funding Science EEIG, Art185), funded jointly by EU and Innovation Fund Denmark.

CRediT authorship contribution statement

Daniel Taylor: Conceptualization, Methodology, Validation, Formal analysis, Investigation, Data curation, Writing - original draft, Visualization, Project administration. **Janus Larsen:** Methodology, Software, Writing - review & editing. **Anna-Lucia Buer:** Investigation, Data curation, Writing - review & editing. **Rene Friedland:** Investigation, Resources, Writing - review & editing. **Andreas Holbach:** Methodology, Data curation, Writing - review & editing. **Jens Kjerulf Petersen:** Project administration, Resources, Funding acquisition, Writing - review & editing. **Pernille Nielsen:** Project administration, Funding acquisition, Writing - review & editing. **Lukas Ritzenhofen:** Investigation, Data curation, Writing - review & editing. **Camille Saurel:** Conceptualization, Project administration, Funding acquisition, Writing - review & editing. **Marie Maar:** Conceptualization, Methodology, Validation, Formal analysis, Investigation, Visualization, Software, Resources, Funding acquisition, Writing - original draft.

Declaration of Competing Interest

The authors declare that they have no known competing financial interests or personal relationships that could have appeared to influence the work reported in this paper.

Acknowledgments

We acknowledge the Latvian Institute of Aquatic Ecology and the Baltic Blue Growth project for sharing mussel growth data from the Latvian farm. We thank the technical staff at the Danish Shellfish Center for assistance in carrying out field measurements and development of monitoring technology. We acknowledge Blå Biomasse A/S, Hjarnø Havbrug, Seafood Limfjord, and Witterup Seafood for access to their farms. We thank Maren Lyngsgaard for resources contributed in relation to data collection at the Venø Sund farm. We thank Xaver Lange (IOW) and Sven Dahlke (Greifswald University) for assistance in carrying out field measurements at GWB. Lastly, we thank the two anonymous reviewers for their very constructive commentary, which contributed to the quality and relevance of the manuscript.

Appendix A. Supplementary data

Supplementary data to this article can be found online at https://doi.org/10.1016/j.ecolind.2020.107304.

References

Backer, H., Leppänen, J.-M., Brusendorff, A.C., Forsius, K., Stankiewicz, M., Mehtonen, J., Pyhälä, M., Laamanen, M., Paulomäki, H., Vlasov, N., Haaranen, T., 2010. HELCOM Baltic Sea Action Plan – A regional programme of measures for the marine environment based on the Ecosystem Approach. Mar. Pollut. Bull. 60, 642–649. https://doi.org/10.1016/j.marpolbul.2009.11.016.

Baddeley, A., Rubak, E., Turner, R., 2015. Spatial Point Patterns: Methodology and Applications with R. Chapman and Hall/CRC Press, London.

Baltic Blue Growth Project, 2019. Baltic Blue Growth: Initiating large scale mussel farming in the Baltic Sea.

Bivand, R.S., Pebesma, E.J., Gómez-Rubio, V., 2013. Applied Spatial Data Analysis with R.

Boesch, D.F., 2019. Barriers and Bridges in Abating Coastal Eutrophication. Front. Mar. Sci. 6, 123. https://doi.org/10.3389/fmars.2019.00123.

Borja, A., Elliott, M., Andersen, J.H., Cardoso, A.C., Carstensen, J., Ferreira, J.G., Heiskanen, A.-S., Marques, J.C., Neto, J.M., Teixeira, H., Uusitalo, L., Uyarra, M.C., Zampoukas, N., 2013. Good Environmental Status of marine ecosystems: What is it and how do we know when we have attained it? Mar. Pollut. Bull. 76, 16–27. https://doi.org/10.1016/J.MARPOLBUL.2013.08.042.

Bricker, S.B., Ferreira, J.G., Simas, T., 2003. An integrated methodology for assessment of estuarine trophic status. Ecol. Model. 169, 39–60. https://doi.org/10.1016/S0304-3800(03)00199-6.

Bricker, S.B., Rice, K.C., Bricker, O.P., 2014. From Headwaters to Coast: Influence of Human Activities on Water Quality of the Potomac River Estuary. Aquat. Geochem. 20, 291–323. https://doi.org/10.1007/s10498-014-9226-y.

Buer, A.L., Maar, M., Nepf, M., Ritzenhofen, L., Dahlke, S., Friedland, R., Krost, P., Piene, F., Schernewski, G., 2020. Potential and feasibility of Mytilus spp. farming along a salinity gradient. Front. Mar. Sci. (In press).

Cloern, J.E., 2018. Why large cells dominate estuarine phytoplankton. Limnol. Oceanogr. 63, S392–S409. https://doi.org/10.1002/lno.10749.

Conley, D.J., Carstensen, J., Aigars, J., Axe, P., Bonsdorff, E., Eremina, T., Haahti, B.-M., Humborg, C., Jonsson, P., Kotta, J., Lännegren, C., Larsson, U., Maximov, A., Medina, M.R., Lysiak-Pastuszak, E., Remeikaité-Nikienė, N., Walve, J., Wilhelms, S., Zillén, L., 2011. Hypoxia is increasing in the coastal zone of the Baltic Sea. Environ. Sci. Technol. 45, 6777–6783. https://doi.org/10.1021/es201212r.

Cranford, P.J., 2019. Magnitude and Extent of Water Clarification Services Provided by Bivalve Suspension Feeding. In: Smaal, A.C., Ferreira, J.G., Grant, J., Petersen, J.K., Strand, Ø. (Eds.), Goods and Services of Marine Bivalves. Springer International Publishing, Cham, pp. 119–141. https://doi.org/10.1007/978-3-319-96776-9_8.

Cranford, P.J., Duarte, P., Robinson, S.M.C., Fernández-Reiriz, M.J., Labarta, U., 2014. Suspended particulate matter depletion and flow modification inside mussel (Mytilus galloprovincialis) culture rafts in the Ría de Betanzos. Spain. J. Exp. Mar. Biol. Ecol. 452, 70–81. https://doi.org/10.1016/j.jembe.2013.12.005.

Cranford, P.J., Strohmeier, T., Filgueira, R., Strand, Ø., 2016. Potential methodological influences on the determination of particle retention efficiency by suspension feeders: Mytilus edulis and ciona intestinalis. Aquat. Biol. 25, 61–73. https://doi.org/10.3354/ab00660.

Cranford, P.J., Ward, J.E., Shumway, S.E., 2011. Bivalve fi lter feeding : variability and limits of the aquaculture biofi lter 81–124.

Cribari-Neto, F., Zeileis, A., 2010. Beta Regression in R. J. Stat. Softw. 34, 1–24.

Dale L. Zimmerman, Michael Stein, 2010. Classical Geostatistical Methods, in: Handbook of Spatial Statistics. CRC Press. https://doi.org/10.1201/9781420072884-c3.

Dolmer, P., 2000. Feeding activity of mussels Mytilus edulis related to near-bed currents and phytoplankton biomass. J. Sea Res. https://doi.org/10.1016/S1385-1101(00)00052-6.

Duarte, C.M., Krause-Jensen, D., 2018. Intervention Options to Accelerate Ecosystem Recovery From Coastal Eutrophication. Front. Mar. Sci. 5, 470. https://doi.org/10.3389/fmars.2018.00470.

Fegley, S.R., MacDonald, B.A., Jacobsen, T.R., 1992. Short-term variation in the quantity and quality of seston available to benthic suspension feeders. Estuar. Coast. Shelf Sci. 34, 393–412. https://doi.org/10.1016/S0272-7714(05)80078-2.

Ferrari, S., Cribari-Neto, F., 2004. Beta Regression for Modelling Rates and Proportions. J. Appl. Stat. 31, 799–815. https://doi.org/10.1080/0266476042000214501.

Ferreira, J.G., Andersen, J.H., Borja, A., Bricker, S.B., Camp, J., Cardoso da Silva, M., Garcés, E., Heiskanen, A.-S., Humborg, C., Ignatiades, L., Lancelot, C., Menesguen, A., Tett, P., Hoepffner, N., Claussen, U., 2011. Overview of eutrophication indicators to assess environmental status within the European Marine Strategy Framework Directive. Estuar. Coast. Shelf Sci. 93, 117–131. https://doi.org/10.1016/j.ecss.2011.03.014.

Ferreira, J.G., Hawkins, A.J.S., Bricker, S.B., 2007. Management of productivity, environmental effects and profitability of shellfish aquaculture - the Farm Aquaculture Resource Management (FARM) model. Aquaculture 264, 160–174. https://doi.org/10.1016/j.aquaculture.2006.12.017.

Ferreira, J.G., Hawkins, A.J.S., Monteiro, P., Moore, H., Service, M., Pascoe, P.L., Ramos, L., Sequeira, A., 2008. Integrated assessment of ecosystem-scale carrying capacity in shellfish growing areas. Aquaculture 275, 138–151. https://doi.org/10.1016/j.aquaculture.2007.12.018.

Filgueira, R., Comeau, L.A., Guyondet, T., McKindsey, C.W., Byron, C.J., 2015. Modelling Carrying Capacity of Bivalve Aquaculture: A Review of Definitions and Methods. In: Meyers, R.A. (Ed.), Encyclopedia of Sustainability Science and Technology. Springer, New York, New York, NY, pp. 1–33. https://doi.org/10.1007/978-1-4939-2493-6_945-1.

Filgueira, R., Grant, J., Petersen, J.K., 2018. Identifying the optimal depth for mussel suspended culture in shallow and turbid environments. J. Sea Res. 132, 15–23. https://doi.org/10.1016/j.seares.2017.11.006.

Fleming-Lehtinen, V., Andersen, J.H., Carstensen, J., Łysiak-Pastuszak, E., Murray, C., Pyhälä, M., Laamanen, M., 2015. Recent developments in assessment methodology reveal that the Baltic Sea eutrophication problem is expanding. Ecol. Indic. 48, 380–388. https://doi.org/10.1016/j.ecolind.2014.08.022.

Fleming-Lehtinen, V., Laamanen, M., 2012. Long-term changes in Secchi depth and the role of phytoplankton in explaining light attenuation in the Baltic Sea. Estuar. Coast. Shelf Sci. 102–103, 1–10. https://doi.org/10.1016/j.ecss.2012.02.015.

Friedland, R., Buer, A.-L., Dahlke, S., Schernewski, G., 2019a. Spatial Effects of Different Zebra Mussel Farming Strategies in an Eutrophic Baltic Lagoon. Front. Environ. Sci. 6, 158. https://doi.org/10.3389/fenvs.2018.00158.

Friedland, R., Schernewski, G., Gräwe, U., Greipsland, I., Palazzo, D., Pastuszak, M., 2019b. Managing Eutrophication in the Szczecin (Oder) Lagoon-Development, Present State and Future Perspectives. Front. Mar. Sci. 5, 521. https://doi.org/10.3389/fmars.2018.00521.

Garmendia, M., Borja, A., Franco, J., Revilla, M., 2013. Phytoplankton composition indicators for the assessment of eutrophication in marine waters: Present state and challenges within the European directives. Mar. Pollut. Bull. 66, 7–16. https://doi.org/10.1016/j.marpolbul.2012.10.005.

Gibbs, M.T., 2007. Sustainability performance indicators for suspended bivalve aquaculture activities. Ecol. Indic. 7, 94–107. https://doi.org/10.1016/j.ecolind.2005.10.004.

Gosling, E., 2015. How bivalves feed. Mar. Bivalve Molluscs 99–156. https://doi.org/10.1002/9781119045212.ch4.

Grant, J., Filgueira, R., 2011. The Application of Dynamic Modeling to Prediction of Production Carrying Capacity in Shellfish Farming. In: Shellfish Aquaculture and the Environment. John Wiley & Sons Ltd, pp. 135–154. https://doi.org/10.1002/9780470960967.ch6.

Grant, J., Pastres, R., 2019. Ecosystem Models of Bivalve Aquaculture: Implications for Supporting Goods and Services. In: Smaal, A.C., Ferreira, J.G., Grant, J., Petersen, J. K., Strand, Ø. (Eds.), Goods and Services of Marine Bivalves. Springer International Publishing, Cham, pp. 507–525. https://doi.org/10.1007/978-3-319-96776-9_25.

Gribov, A., Krivoruchko, K., 2020. Empirical Bayesian kriging implementation and usage. Sci. Total Environ. 722, 137290 https://doi.org/10.1016/j.scitotenv.2020.137290.

Guyondet, T., Roy, S., Koutitonsky, V.G., Grant, J., Tita, G., 2010. Integrating multiple spatial scales in the carrying capacity assessment of a coastal ecosystem for bivalve aquaculture. J. Sea Res. 64, 341–359. https://doi.org/10.1016/j.seares.2010.05.003.

Harvey, E.T., Walve, J., Andersson, A., Karlson, B., Kratzer, S., 2019. The Effect of Optical Properties on Secchi Depth and Implications for Eutrophication Management. Front. Mar. Sci. 5, 496. https://doi.org/10.3389/fmars.2018.00496.

HELCOM, 2013. HELCOM Copenhagen Ministerial Declaration: Taking Further Action to Implement the Baltic Sea Action Plan-Reaching a Good Environmental Status for a Healthy Baltic Sea.

HELCOM, 2007. Baltic Sea Action Plan. HELCOM Ministerial Meeting, Krakow, Poland.

Hofmeister, R., Burchard, H., Bolding, K., 2009. A three-dimensional model study on processes of stratification and de-stratification in the Limfjord. Cont. Shelf Res. https://doi.org/10.1016/j.csr.2009.04.004.

Holbach, A., Maar, M., Timmermann, K., Taylor, D., 2020. A spatial model for nutrient mitigation potential of blue mussel farms in the western Baltic Sea. Sci. Total Environ. 736, 139624 https://doi.org/10.1016/j.scitotenv.2020.139624.

Holbach, A., Wang, L., Chen, H., Hu, W., Schleicher, N., Zheng, B., Norra, S., 2013. Water mass interaction in the confluence zone of the Daning River and the Yangtze River—a driving force for algal growth in the Three Gorges Reservoir. Environ. Sci. Pollut. Res. 20, 7027–7037. https://doi.org/10.1007/s11356-012-1373-3.

Holm-Hansen, O., Lorenzen, C.J., Holmes, R.W., Strickland, J.D.H., 1965. Fluorometric determination of chlorophyll. ICES J. Mar. Sci. 30, 3–15. https://doi.org/10.1093/icesjms/30.1.3.

Hulot, V., Saulnier, D., Lafabrie, C., Gaertner-Mazouni, N., 2018. Shellfish culture: a complex driver of planktonic communities. Rev. Aquac. 12, 33–46. https://doi.org/10.1111/raq.12303.

Jansen, H.M., Reid, G.K., Bannister, R.J., Husa, V., Robinson, S.M.C., Cooper, J.A., Quinton, C., Strand, Ø., 2016. Discrete water quality sampling at open-water aquaculture sites: limitations and strategies. Aquac. Environ. Interact. 8, 463–480.

Kirk, J.T.O., 2011. Light and photosynthesis in aquatic ecosystems. Cambridge University Press, Cambridge, UK, New York.

Kooijman, S.A.L.M., 2010. Dynamic Energy and Mass Budgets in Biological Systems. Dynamic Energy and Mass Budgets in Biological Systems. https://doi.org/10.1017/cbo9780511565403.

Kristensen, P., Whalley, C., Zal, F.N.N., Christiansen, T., 2018. European Waters Assessment of Status and Pressures 2018, European Environment Agency. https://doi.org/10.2800/303664.

Krivoruchko, K., Gribov, A., 2019. Evaluation of empirical Bayesian kriging. Spat. Stat. 32, 100368 https://doi.org/10.1016/j.spasta.2019.100368.

Larsen, J., Mohn, C., Pastor, A., Maar, M., 2020. A versatile marine modelling tool applied to arctic, temperate and tropical waters. PLoS ONE 15, e0231193. https://doi.org/10.1371/journal.pone.0231193.

Lind, O.T., 1986. The effect of non-algal turbidity on the relationship of Secchi depth to chlorophyll a. Hydrobiologia 140, 27–35. https://doi.org/10.1007/BF00006726.

Maar, M., Bolding, K., Petersen, J.K., Hansen, J.L.S., Timmermann, K., 2009. Local effects of blue mussels around turbine foundations in an ecosystem model of Nysted off-shore wind farm, Denmark. Metab. Organ. 30 Years DEB Appl. Dev. 62, 159–174. https://doi.org/10.1016/j.seares.2009.01.008.

Maar, M., Larsen, M.M., Tørring, D., Petersen, J.K., 2018. Bioaccumulation of metals (Cd, Cu, Ni, Pb and Zn) in suspended cultures of blue mussels exposed to different environmental conditions. Vectors Change Mar. Environ. 201, 185–197. https://doi.org/10.1016/j.ecss.2015.10.010.

Maar, M., Saurel, C., Landes, A., Dolmer, P., Petersen, J.K., 2015. Growth potential of blue mussels (M. edulis) exposed to different salinities evaluated by a Dynamic Energy Budget model. J. Mar. Syst. 148, 48–55. https://doi.org/10.1016/j.jmarsys.2015.02.003.

Miljø- og Fødevareministeriet, 2016. Vandområdeplan 2015-2021 for Vandområdedistrikt Jylland og Fyn.

Møhlenberg, F., Riisgård, H.U., 1978. Efficiency of particle retention in 13 species of suspension feeding bivalves. Ophelia 17, 239–246. https://doi.org/10.1080/00785326.1978.10425487.

Newell, C., Hawkins, A.J.S., Morris, K., Richardson, J., Davis, C., Getchis, T., 2013. ShellGIS: a dynamic tool for shellfish farm site selection. Wold Aquac. 44, 50–53.

Newell, C.R., Brady, D.C., Richardson, J., 2019. Farm-Scale Production Models. In: Smaal, A.C., Ferreira, J.G., Grant, J., Petersen, J.K., Strand, Ø. (Eds.), Goods and Services of Marine Bivalves. Springer International Publishing, Cham, pp. 485–506. https://doi.org/10.1007/978-3-319-96776-9_24.

Newell, C.R., Richardson, J., 2014. The Effects of Ambient and Aquaculture Structure Hydrodynamics on the Food Supply and Demand of Mussel Rafts. J. Shellfish Res. 33, 257–272. https://doi.org/10.2983/035.033.0125.

Ní Longphuirt, S., McDermott, G., O'Boyle, S., Wilkes, R., Stengel, D.B., 2019. Decoupling Abundance and Biomass of Phytoplankton Communities Under Different Environmental Controls: A New Multi-Metric Index. Front. Mar. Sci. 6, 312. https://doi.org/10.3389/fmars.2019.00312.

Nielsen, P., Cranford, P.J., Maar, M., Petersen, J.K., 2016. Magnitude, spatial scale and optimization of ecosystem services from a nutrient extraction mussel farm in the eutrophic Skive Fjord. Denmark. Aquac. Environ. Interact. 8, 311–329. https://doi.org/10.3354/aei00175.

Oksanen, J., Blanchet, F.G., Friendly, M., Kindt, R., Legendre, P., McGlinn, D., Minchin, P.R., O'Hara, R.B., Simpson, G.L., Solymos, P., Stevens, M.H.H., Szoecs, E., Wagner, H., 2019. vegan: Community Ecology Package.

Petersen, Jens Kjerulf, Holmer, M., Termansen, M., Hasler, B., 2019a. Nutrient Extraction Through Bivalves. In: Smaal, A.C., Ferreira, J.G., Grant, J., Petersen, Jens K, Strand, Ø. (Eds.), Goods and Services of Marine Bivalves. Springer International Publishing, Cham, pp. 179–208. https://doi.org/10.1007/978-3-319-96776-9_10.

Petersen, J.K., Loo, L.-O., Taylor, D., 2019b. Evaluating chlorophyll depletion in mitigation mussel cultivation at multiple scales. Aquac. Environ. Interact. https://doi.org/10.3354/aei00312.

Petersen, J.K., Nielsen, T.G., van Duren, L., Maar, M., 2008. Depletion of plankton in a raft culture of Mytilus galloprovincialis in Ría de Vigo, NW Spain. I. Phytoplankton. Aquat. Biol. 4, 113–125. https://doi.org/10.3354/ab00124.

Pilz, J., Spöck, G., 2008. Why do we need and how should we implement Bayesian kriging methods. Stoch. Environ. Res. Risk Assess. 22, 621–632. https://doi.org/10.1007/s00477-007-0165-7.

Plew, D.R., 2011. Depth-Averaged Drag Coefficient for Modeling Flow through Suspended Canopies. J. Hydraul. Eng. 137, 234–247. https://doi.org/10.1061/(ASCE)HY.1943-7900.0000300.

Riisgård, H.U., Kittner, C., Seerup, D.F., 2003. Regulation of opening state and filtration rate in filter-feeding bivalves (Cardium edule, Mytilus edulis, Mya arenaria) in response to low algal concentration. J. Exp. Mar. Biol. Ecol. 284, 105–127. https://doi.org/10.1016/S0022-0981(02)00496-3.

Rosa, M., Ward, J., Shumway, S., 2018. Selective Capture and Ingestion of Particles by Suspension-Feeding Bivalve Molluscs: A Review. J. Shellfish Res. 37, 727–746. https://doi.org/10.2983/035.037.0405.

Rosland, R., Bacher, C., Strand, Ø., Aure, J., Strohmeier, T., 2011. Modelling growth variability in longline mussel farms as a function of stocking density and farm design. J. Sea Res. 66, 318–330. https://doi.org/10.1016/j.seares.2011.04.009.

Schröder, T., Stank, J., Schernewski, G., Krost, P., 2014. The impact of a mussel farm on water transparency in the Kiel Fjord. Ocean Coast. Manag. 101, 42–52. https://doi.org/10.1016/j.ocecoaman.2014.04.034.

Smaal, A.C., van Duren, L.A., 2019. Bivalve Aquaculture Carrying Capacity: Concepts and Assessment Tools, in: Smaal, A.C., Ferreira, J.G., Grant, J., Petersen, J.K., Strand, Ø. (Eds.), Goods and Services of Marine Bivalves. Springer International Publishing, Cham, pp. 451–483. https://doi.org/10.1007/978-3-319-96776-9_23.

Stevens, C., Plew, D., 2019. Bridging the Separation Between Studies of the Biophysics of Natural and Built Marine Canopies. Front. Mar. Sci. 6, 217. https://doi.org/10.3389/fmars.2019.00217.

Stevens, C.L., Petersen, J.K., 2011. Turbulent, stratified flow through a suspended shellfish canopy: Implications for mussel farm design. Aquac. Environ. Interact. 2, 87–104. https://doi.org/10.3354/aei00033.

Strand, Ø., Ferreira, J.G., 2019. Introduction to Regulating Services. In: Smaal, A.C., Ferreira, J.G., Grant, J., Petersen, J.K., Strand, Ø. (Eds.), Goods and Services of Marine Bivalves. Springer International Publishing, Cham, pp. 115–117. https://doi.org/10.1007/978-3-319-96776-9_7.

Strohmeier, T., Duinker, A., Strand, Ø., Aure, J., 2008. Temporal and spatial variation in food availability and meat ratio in a longline mussel farm (Mytilus edulis). Aquaculture 276, 83–90. https://doi.org/10.1016/J.AQUACULTURE.2008.01.043.

Taylor, D., Saurel, C., Nielsen, P., Petersen, J.K., 2019. Production Characteristics and Optimization of Mitigation Mussel Culture. Front. Mar. Sci. 6, 698. https://doi.org/10.3389/fmars.2019.00698.

Timmermann, K., Maar, M., Bolding, K., Larsen, J., Windolf, J., Nielsen, P., Petersen, J. K., 2019. Mussel production as a nutrient mitigation tool for improving marine water quality. Aquacult. Environ. Interact. https://doi.org/10.3354/aei00306.

Tseung, H.L., Kikkert, G.A., Plew, D., 2016. Hydrodynamics of suspended canopies with limited length and width. Environ. Fluid Mech. 16, 145–166. https://doi.org/10.1007/s10652-015-9419-y.

van der Veer, H.W., Cardoso, J.F.M.F., van der Meer, J., 2006. The estimation of DEB parameters for various Northeast Atlantic bivalve species. J. Sea Res. https://doi.org/10.1016/j.seares.2006.03.005.

von Thenen, M., Maar, M., Hansen, H.S., Friedland, R., Schiele, K.S., 2020. Applying a combined geospatial and farm scale model to identify suitable locations for mussel farming. Mar. Pollut. Bull. In Press.

Weitzman, J., Filgueira, R., 2020. The evolution and application of carrying capacity in aquaculture: towards a research agenda. Rev. Aquac. 12, 1297–1322. https://doi.org/10.1111/raq.12383.

Winder, M., Carstensen, J., Galloway, A.W.E., Jakobsen, H.H., Cloern, J.E., 2017. The land–sea interface: A source of high-quality phytoplankton to support secondary production. Limnol. Oceanogr. 62, S258–S271. https://doi.org/10.1002/lno.10650.